

We would like to thank both reviewers for their follow-up and constructive comments that helped to improve the manuscript further.

Please find below the reviewer's comments in regular italic and a point-by-point description of additional changes in bold font. Comments from the last round are given in light grey.

Reviewer 1

The authors have (nearly) addresses all my points raised in my initial review and made a good effort to improve the manuscript. I like the appendix on the NH ice sheet reconstruction approach and I think that the experiments as well as the results are now presented in a more comprehensive way. Nevertheless, I still have a few points I urge the authors to address before this manuscript goes in print.

We would like to thank reviewer 1 for the additional comments. We are confident that addressing these comments and those of reviewer 2 has improved the manuscript sufficiently for publication.

C: Ice volume/sea level curve which corresponds to implemented ice sheets

Relating to the previous comment B I am missing a figure with the 135ka-120ka ice volume/sea level equivalent for Greenland, Antarctica, the NH ice sheets, and their sum to complement Fig. 3. As the authors claim to force LOVECLIM with realistic ice sheet boundary conditions (e.g., stated on page 4406, line 14) this ice sheet volume/ sea level curve used for the "Reference" experiment should be validated with an observational reference (e.g., Kopp et al., 2009). A respective figure would be very helpful for the reader and illustrate the descriptions on page 4397, lines 16-27.

We agree that such a figure would be in place here. However, we have a companion paper in CPD (Goelzer et al., 2016), which complements the present work with specific focus on the sea-level reconstruction of the LIG period. We have therefore decided to only add a reference to the other work with focus on this specific problem:

"More details about the sea-level evolution can be found in a companion paper (Goelzer et al., 2016) that specifically deals with the sea-level contribution of the ice sheets during the LIG in a fully coupled model set-up. "

1. Follow-up to point C in the initial review (and your answer given):

I am ok with that you don't want to discuss the sea level changes in full details to avoid duplication with Goelzer et al., 2016. Nevertheless, I think a figure (e.g., panel added to Fig. 3) showing the LIG evolution in ice volume for the NH, GrlS, and AIS is of crucial importance.

You have several statements in the text referring to the state/changes of the ice sheets during the LIG and the reader is tempted to derive these ice sheet changes from the FWFs in Fig. 3. Thus, in the current form this can lead to misunderstandings, as happened in my case (see point C in initial review). You should therefore make it clearer how the shape of the FWF curves in Fig. 3 connect to the ice sheet changes and I am convinced that this is best done by showing the ice volume changes as a figure as well.

We have followed the suggestion and have included additional panels in Figure 3 showing the ice volume evolution of the NH ice sheets, GrIS and AIS. References in the text have been updated accordingly.

I am curious if the Antarctic ice volume is growing from 125ka to 120ka as implied by Fig. 2. This seems to be in contrast with the ongoing Antarctic FWF throughout the LIG (Fig. 3b) which I connect with a retreating ice sheet.

The volume of the ice sheet does grow between 125 kyr and 120 kyr BP. However, there is always a flux of freshwater from the ice sheet from ice and meltwater discharge into the ocean, irrespective of the change in ice volume. We believe there is a misunderstanding based on the confusion between freshwater flux and net total mass balance. See also next point D.

D: Questions regarding FWF (Fig. 3)

Moreover, I feel I have to question the massive Antarctic FWF between 128ka and 120ka. A rough calculation for 8000 years of 0.1Sv is equal to a global sea-level rise of ~70m - is this totally balanced by evaporation from the oceans or any other process?

As mentioned in response to the last point, we show in Fig. 3 the actual freshwater flux from the ice sheets to the ocean. The ocean model has an implicit free surface meaning that the surface freshwater fluxes can be explicitly taken into account. Nevertheless, for simulations with that large amount of freshwater input, there is an option to conserve global salinity and global ocean volume to avoid problems, which is applied here.

2. Follow-up to point D in my initial review (and your answer given) #1:

I am fully aware of the fact that FWF are only one component of the net surface balance of the AIS. Still, I wonder whether the 0.4 Sv peak and the ~constant 0.1 Sv flux throughout the LIG are reasonable estimates (at least in terms of magnitude). This question has not been answered in your author response. How do your AIS FWFs compare with present-day FWFs?

A recent estimate of the present-day net precipitation (snowfall+rainfall) on the entire area of the AIS is ~2700 Gt/year (Lenaerts et al., 2012). If the ice sheet were in equilibrium, this would translate to a FWF of ~0.085 Sv. With modeled accumulation slightly higher during LIG compared to present (Goelzer et al., 2016), our modeled LIG background

flux of ~0.1 Sv is in good agreement with what can be expected from reconstructions. The peak FWF of ~0.4 Sv is physically controlled by the modelled rate of ice sheet retreat and by the total glacial-interglacial ice volume contrast. Both factors are not well constrained by reconstructions. We had therefore already included a schematic control run with Antarctic FWF scaled by 50 % in the discussion of the original manuscript. We have now included a comment in the manuscript to better motivate this experiment in relation to the uncertainties stated above.

Goelzer, H., Huybrechts, P., Loutre, M. F. and Fichet, T.: Last Interglacial climate and sea-level evolution from a coupled ice sheet-climate model, *Climate of the Past Discussions*, 1–34, doi:10.5194/cp-2015-175-EC2, 2016.

Lenaerts, J. T. M., van den Broeke, M. R., van de Berg, W. J., van Meijgaard, E. and Kuipers Munneke, P.: A new, high-resolution surface mass balance map of Antarctica (1979-2010) based on regional atmospheric climate modeling, *Geophys Res Lett*, 39(4), n/a–n/a, doi:10.1029/2011GL050713, 2012.

3. *Follow-up to point D in my initial review (and your answer given) #2:*

You mention in the author response that you choose the ocean model to conserve global ocean salinity and ocean volume despite adding substantial amounts of FWF. This should definitely be mentioned in the manuscript and implications of the resulting physical inconsistency need to be discussed.

OK. This is now mentioned in the model description:

“As common practice for simulations with large amounts of freshwater input, we conserve global salinity and global volume in the ocean model to avoid numerical problems.”

4. *Please do another careful editorial check of the whole manuscript. In particular regarding references and abbreviations used in the manuscript, I quickly spotted several errors/inconsistencies. Some examples are:*

OK. We have checked and corrected all references and abbreviations in the manuscript. Aside from the examples from the reviewer we have updated references Letréguilly et al. (1991); Pépin et al. (2001); Sánchez Goñi et al. (2012); van de Berg et al. (2013); Zweck and Huybrechts (2003).

- (GHG) should be introduced at first instance (page 6, line 183)

OK.

- NH and SH abbreviations should be used consistently instead of the full “Northern Hemisphere / Southern Hemisphere as those are very common terms. On page 16, line 472: “northern hemisphere” should be NH or at least

“Northern Hemisphere”,

- same in caption of Fig. A1

OK. We now use the abbreviations throughout the manuscript, except for figure captions and section titles. We have replaced “northern hemisphere” by “NH” or “Northern Hemisphere” in all instances.

- The use of “present-day” and “present day” is not consistent throughout the manuscript

OK.

- “Clague and James 2001” should be “Clague and James 2002”

OK. Thank you for spotting this one.

- Stuiver et al. 1998 is referenced in text but not in the reference list

OK.

Wording

1. Page 1, line 23-26 (Abstract): This sentence sounds a little odd to me. May be add “as well” after “which are modulated” to make it clearer.

OK, reformulated to “which are additionally modulated by the direct impact of Antarctic meltwater fluxes”.

2. Page 2, Lines 53-56: Again I find this sentence a bit confusing. Please be clearer on what you mean with “relatively short period” and provide specific time ranges.

OK, replaced “in a relatively short period” by “during Termination II”.

3. Page 4, line 2: add “, particularly in the SH” after “on the climate”. This makes it clearer that your main focus is on the climate evolution in the SH.

OK.

4. Page 8, lines 228-230: This sentence is only partly clear to me. Why are the air temperatures in all runs similar when the FWF of all ice sheets are similar? Please clarify.

OK. We have changed the end of the sentence to “and FWF are similar between the different experiments.” to clarify that we discuss differences between experiments not differences between ice sheets.

“Global mean and hemispheric mean temperatures are similar in all runs after ~127 kyr BP, when the ice sheets have largely reached their interglacial configuration and FWF are similar between the different experiments.”

5. Page 8, line 243: I think “warming trends” is not the appropriate term here.

OK, reformulated.

“The strong warming in the ice sheet periphery is due to a combination of ...”

6. Page 8, line 247: add “(not shown)” after “WAIS”.

OK.

Reviewer 2

The manuscript clearly improved from its last version. It is, however, still not ready for publication. Some results are not clearly presented, and some essential information is still lacking. Please find below my minor comments that will hopefully improve the readability of the manuscript. Please also go through the entire text and rewrite to be more concise.

We would like to thank reviewer 2 for the detailed comments. We have revised the entire manuscript once more to remove remaining inconsistencies. We are confident that addressing the comments of both reviewers has improved the manuscript sufficiently.

Specific comments:

Northern Hemisphere ice sheet forcing/Appendix A: In the last version of the manuscript there was too few information, now there is too much. Please rewrite to be more concise, and exact. Suggestions for some changes:

We have revised and shortened the Appendix to reflect the reviewers’ suggestions and make the description more concise.

Line 465: Appendix A

OK.

Line 469-470 and following: what is the difference between post-LGM and Termination I? Maybe better to change all to Termination I?

OK, changed to Termination I. This has also been done everywhere else in the manuscript.

Line 472: change to NH

OK.

Lines 482-483: change ‘more’ to ‘most’

OK.

Lines 496-497: change to ‘... Figure A1, neglecting isostatic adjustment (i.e. using present...)

OK.

Lines 500-502: rewrite

OK, reformulated:

“The basal shear stress for the parabolic profile reconstruction is chosen so that the difference in ice volume between LGM and PD corresponds to 86 m of eustatic sea level change. With isostasy accounted for, a similar elevation would result in an additional contribution of 24 m to a total equivalent eustatic sea level change of 110 m (cf. Zweck and Huybrechts, 2005). ”

The important part here is the remapping of post-LGM/Termination I retreat to Termination II, which is based on the d18O record of Lisiecki and Raymo (2005). How similar are these two terminations in the d18O record? And is reshuffling of the Termination I records a valid approach?

As already discussed in the manuscript, information about Termination II is very limited. Assuming similar ice sheet configuration for similar (d18O value interpreted as) global ice volume is to our knowledge the best data based guess we can currently make. The d18O record looks similar between the two terminations, but that is unlikely to validate or invalidate our approach.

Line 121: explain MIS 5e, or change to LIG

OK, changed to LIG.

Line 130: delete Stone reference here; they don’t use the index method

OK.

Line 135: delete first ‘as’

OK.

Lines 147-154: The approach of using the two different sea-level curves still does not make sense to me. I understand that the GrlS is not largely influenced by using another record, but it is confusing that the AIS is forced directly by the Grant sea level reconstruction, and at the same time indirectly by the FWF from the NH ice sheets that are reconstructed using the LR05 stack. This is especially important because of the different timing of the sea level highstand in both reconstructions. Please discuss.

Using a sea-level record with a good chronology as forcing for the AIS is crucial because the ice sheet response directly depends on it. We have therefore excluded LR05 for this purpose and use the Grant record. In earlier work (Loutre et al., 2014) we have tried to use the Grant record for

the NH ice sheet reconstruction but had to conclude that LR05 gave much better results for the modelled climate response. We have discussed several additional lines of evidence for a good NH ice sheet reconstruction using LR05 in the present manuscript.

We have included an additional sentence in the discussion to clarify this:

“Reconstructing the NH ice sheet evolution during Termination II with the same method but using the Grant et al. (2012) sea-level record for comparison with Termination I has been shown to worsen agreement of the modelled climate with proxy reconstructions (Loutre et al., 2014).”

Lines 159-160: change ‘In that case’, to ‘Therefore’

OK, has been changed.

Lines 161-162: Change to: ‘The FWF from the dynamic GrIS and AIS replace...’

OK, has been changed.

Lines 165-177: As suggested before, I still think a figure comparing your sea level contributions to the Kopp et al. (2009) data is necessary. Your companion paper deals with a fully coupled climate and ice sheet model, so likely the sea level will be different from the one prescribed here. As the sea level evolution is essential for the results of the present study, it really should be clearly shown and discussed.

We have followed the suggestion of reviewer 1 to include the ice volume evolution of the NH ice sheets, GrIS and AIS as additional panels in Figure 3.

Lines 208-210: rewrite

OK, reformulated:

“Including the forcing from the NH ice sheets in terms of configuration and FWF has been shown by Loutre et al. (2014) to be crucial to simulate the onset of the LIG temperature increase and its amplitude variations more in line with proxy records.”

Lines 213-214: Change to: ‘The increased temperature changes of these simulations is due to albedo...’

OK, reformulated. It is important to distinguish “our” simulations from “these” simulations mentioned just before without NH forcing, hence the following modification:

“The increased amplitude of temperature changes in our simulations is due to albedo and elevation changes”.

Line 230: 'FWF are similar'? Or small?

No change. The *additional* FWF from Greenland is small compared to the other source. Including it (reference) or not (noAG) does not make a big difference.

Line 235: Change to 'Here changes in AMIC cause a perturbation...'

OK, reformulated.

“Here changes in the AMOC cause a perturbation of ...”

Figure 6: Another possible reason for the mismatch could be due to the comparison of modelled temperatures over a large region to local measured anomalies.

The modelled temperature is an average over an area roughly delimited by the deep ice core sites. However, the average shows a similar temperature evolution compared to individual model grid points located at the ice core sites.

Line 261: 'partially suppressed'? Suppressed to PI values? Or no FWF at all?

OK, removed “partially”, which makes the description clearer. The idea was to indicate that e.g. in noGfwf, freshwater fluxes are suppressed only from the GrIS. The freshwater fluxes are completely suppressed (for one ice sheet or the other or both) and results compared to the reference experiment, not to the pre-industrial.

Lines 397-399: delete sentence

OK, deleted.

Line 400: delete “climatic”

OK, deleted.

Impact of ice sheet meltwater fluxes on the climate evolution at the onset of the Last Interglacial

H. Goelzer^{1*}, P. Huybrechts¹, Marie-France Loutre², Thierry Fichefet²

¹Earth System Sciences & Departement Geografie, Vrije Universiteit Brussel, Brussels, Belgium

²Université catholique de Louvain, Earth and Life Institute, Georges Lemaître Centre for Earth and Climate Research (TECLIM), Louvain-la-Neuve, Belgium

*now at: Institute for Marine and Atmospheric research Utrecht, Utrecht University, the Netherlands

Correspondence to: H. Goelzer (heiko.goelzer@vub.ac.be)

Abstract

Large climate perturbations occurred during the transition between the penultimate glacial period and the Last Interglacial (Termination II), when the ice sheets retreated from their glacial configuration. Here we investigate the impact of ice sheet changes and associated freshwater fluxes on the climate evolution at the onset of the Last Interglacial. The period from 135 to 120 kyr BP is simulated with the Earth system model of intermediate complexity LOVECLIM v.1.3 with prescribed evolution of the Antarctic ice sheet, the Greenland ice sheet and the other Northern Hemisphere ice sheets. Variations in meltwater fluxes from the Northern Hemisphere ice sheets lead to North Atlantic temperature changes and modifications of the strength of the Atlantic meridional overturning circulation. By means of the interhemispheric see-saw effect, variations in the Atlantic meridional overturning circulation also give rise to temperature changes in the Southern Hemisphere, which are additionally modulated -by the direct impact of Antarctic meltwater fluxes into the Southern Ocean. Freshwater fluxes from the melting Antarctic ice sheet lead to a millennial time scale oceanic

28 cold event in the Southern Ocean with expanded sea ice as evidenced in some ocean sediment
29 cores, which may be used to constrain the timing of ice sheet retreat.

30

31 **1 Introduction**

32 Understanding the climate and ice sheet evolution during past warm periods in the history of
33 the Earth may provide important insights for projections of future climate and sea-level
34 changes. The growing amount of paleo-reconstructions for the Last Interglacial period (e.g.
35 Govin et al., 2012; Capron et al., 2014) in combination with improved model simulations of
36 this most recent warm period (e.g. Bakker et al., 2013; Lunt et al., 2013, Langebroek and
37 Nisancioglu, 2014; Loutre et al., 2014) make it an interesting target for studying the coupled
38 climate-ice sheet system.

39 According to reconstructions, the Last Interglacial (LIG, from ~130-115 kyr BP) was
40 characterised by a global annual mean surface temperature of up to 2° C above the pre-
41 industrial (e.g. Turney and Jones, 2010; Capron et al., 2014) and a sea-level high stand of 6-9
42 m above the present day (Kopp et al., 2009; Dutton and Lambeck, 2012). As the penultimate
43 glacial maximum was at least as severe as the Last Glacial Maximum (LGM) in both
44 hemispheres (EPICA community members, 2004; Svendsen et al., 2004), this implies a large
45 amplitude glacial-interglacial transition in terms of temperature and ice sheet configuration.
46 At the onset of the LIG, a rapid warming of ~10°C from the preceding cold state is recorded
47 in deep Antarctic ice cores (Masson-Delmotte et al., 2011) to have occurred between ~135
48 kyr BP and 130 kyr BP. Current ice core records from the Greenland ice sheet (GrIS) do not
49 extend long enough back in time to cover the entire penultimate deglaciation and associated
50 warming (NEEM community members, 2013), but a similar timing and magnitude of
51 warming compared to the Antarctic can be reconstructed for sea surface temperatures off the
52 West European margin (~~Sánchez Goñi~~~~Sánchez-Goni~~ et al., 2012). The warming is closely
53 related with an ice sheet retreat in both hemispheres. Despite large uncertainties in
54 reconstructions, the global sea-level stand at 135 kyr BP of as low as -80 m (Grant et al.,
55 2012) is indicative of the large amount of freshwater that entered the ocean in the form of
56 meltwater from the retreating ice sheets ~~over a relatively short period~~during Termination II.
57 Aside from determining the amplitude of sea-level changes, which is the focus of many
58 studies (e.g. Robinson et al., 2011; Stone et al., 2013), the associated climate impacts and

59 possible feedbacks on the ice sheet evolution of this freshwater forcing are an important
60 element for a process understanding of the coupled climate-ice sheet changes at that time.

61 A climatic mechanism that is thought to be directly related to changes in the NH ice sheet
62 freshwater fluxes (FWF) is the interhemispheric see-saw effect (Stocker, 1998) that links SH
63 warming to a weakening of the Atlantic meridional overturning circulation (AMOC). If the
64 see-saw effect was active during the onset of the LIG, NH ice sheet melting during
65 Termination II would have been the cause for a substantial AMOC weakening and NH
66 cooling, while reduced interhemispheric heat transport would have caused a gradual SH
67 warming (Stocker and Johnson 2003). The see-saw mechanism was evoked to explain part of
68 the peak Antarctic warming during the LIG (e.g. Holden et al., 2010; Marino et al., 2015),
69 even though some Southern Ocean (SO) warming was shown by Langebroek and Nisancioglu
70 (2014) to be possible with orbital forcing alone (without NH freshwater forcing). The see-saw
71 mechanism has been speculated to have caused increased Antarctic ice shelf melting and
72 West Antarctic ice sheet (WAIS) retreat (Duplessy et al., 2007). The retreat of the WAIS,
73 which is believed to have been grounded at the edge of the continental shelf during the
74 penultimate glaciation, generated a large anomalous flux of freshwater into the SO. Such
75 freshwater forcing could have had a substantial influence on the SO configuration in terms of
76 sea ice extent and ocean circulation as shown in model experiments for the last deglaciation
77 (Menviel et al., 2011), for future global warming scenarios (Swingedouw et al., 2008) and for
78 the present day (Bintanja et al., 2013). The impact of increased Antarctic FWF is thought to
79 consist of a surface ocean freshening, stratification of the surface ocean and cooling, in turn
80 promoting sea ice growth (e.g. Bintanja et al., 2013) and reduced Antarctic Bottom Water
81 (AABW) formation (Menviel et al., 2011). Recently, Golledge et al. (2014) suggested that
82 such a mechanism might also have provided a feedback on Antarctic ice sheet (AIS) retreat
83 for meltwater pulse 1A during the last glacial-interglacial transition (Termination I), by
84 promoting warming of mid-depth ocean waters that provide additional heat for melting ice
85 shelves.

86 In the present work, we study the effect of evolving ice sheet boundary conditions on the
87 climate, by simulating the climate evolution at the onset and over the course of the LIG with
88 an Earth system model of intermediate complexity (EMIC). The model is forced with realistic
89 ice sheet boundary conditions from offline simulations of ice dynamic models of the AIS and
90 GrIS and reconstructions of the other NH ice sheets. With this study we extend the work of

91 Loutre et al. (2014) by additionally including dynamic ice sheet changes of the GrIS and AIS
92 and focusing on the effect of ice sheet freshwater fluxes on the climate, particularly in the
93 Southern Hemisphere (SH). The model and experimental setup are described in section 2 and
94 3, respectively, followed by results (Sect. 4, 5 and 6), their discussion in section 7 and
95 conclusions (Sect. 8).

96

97 **2 Model description**

98 We use the EMIC LOVECLIM version 1.3, which includes components representing the
99 atmosphere, the ocean and sea ice, the terrestrial biosphere and the ice sheets (cf. Figure 1).
100 The model has been utilised in a large number of coupled climate-ice sheet studies (e.g.
101 Driesschaert et al., 2007; Swingedouw et al., 2008; Goelzer et al., 2011; 2012a; Loutre et al.,
102 2014) and is described in detail in Goosse et al. (2010).

103 In this study, the climate components are forced by time-evolving ice sheet boundary
104 conditions, which are calculated off-line, i.e. uncoupled from the climate evolution. Our
105 modelling approach for the ice sheets consists of a combination of reconstructed NH ice
106 sheets (except the GrIS) based on geomorphological data (Sec. 2.1) and of standalone ice
107 dynamic simulations of the GrIS and AIS (Sec. 2.2). In either case, the boundary conditions
108 provide time evolving topography, ice sheet extent (albedo) and spatially and temporally
109 variable FWF to the climate model. As common practice for simulations with large amounts
110 of freshwater input, we conserve global salinity and global volume in the ocean model to
111 avoid numerical problems.

112 **2.1 Northern Hemisphere ice sheet forcing**

113 We have little geomorphological evidence for Northern Hemisphere (NH) ice sheet evolution
114 during Termination II since it was mostly destroyed by the re-advance leading to the LGM.
115 Therefore, the reconstruction of NH ice sheet evolution for the period of interest is made
116 based on information from the last deglaciation. The method was already described in some
117 detail in Loutre et al. (2014). Nevertheless, we include a more thorough description here
118 (Appendix A). The resulting boundary conditions used to force the climate model consist of a
119 chronology of ice mask and surface elevation changes (Figure 2) and freshwater fluxes
120 (Figure 3ba) over the entire LIG period. Support for the derived chronology of NH ice sheet
121 evolution and their FWF can be found in records of ice-rafted detritus (IRD) from the

122 subpolar North Atlantic (Kandiano et al., 2004; Oppo et al., 2006). These show variability of
123 similar signature during the deglaciation and in particular a last IRD peak at ~128 kyr BP
124 preceding low IRD levels throughout [the MIS-5eLIG](#).

125 **2.2 Simulations of the Greenland and Antarctic ice sheets**

126 For the present study, the climate components are partially forced by results from stand-alone
127 simulations of the GrIS and AIS, which have been adapted from existing ice sheet model
128 experiments (Huybrechts 2002). The configuration of both ice sheet models and the forcing
129 interface follows the description in Goosse et al. (2010) with the following exceptions.
130 Forcing for the ice sheet models is derived from scaling present-day observations of
131 temperature and precipitation with indices based on ice core records, as often done for long-
132 term paleo ice sheet modelling (e.g. Huybrechts, 1990; Letréguilly et al., 1991; Zweck and
133 Huybrechts, 2005; Greve et al., 2011; ~~Stone et al., 2013~~). For the GrIS the forcing record was
134 created following Fürst et al. (2015). We combine a synthesised Greenland $\delta^{18}\text{O}$ record
135 derived from Antarctica Dome C using a bipolar seesaw model (Barker et al., 2011) with the
136 NEEM temperature reconstruction (NEEM community members, 2013) between 128.44 kyr
137 BP and 120 kyr BP. The Barker $\delta^{18}\text{O}$ record is converted to a spatially uniform temperature
138 anomaly with a constant temperature/ isotope factor ~~as~~ $\Delta T = 2.4 \text{ }^\circ\text{C}/\text{‰} * (\delta^{18}\text{O} + 34.83)$ as in
139 Huybrechts (2002). Positive temperature anomalies of the NEEM record are scaled by a factor
140 0.6 to fulfil constraints on maximal ice sheet retreat from Camp Century and Dye3 ice core
141 locations that are assumed to have been ice covered during the LIG. This places the GrIS
142 evolution in the range of former model estimates during that period (e.g. Robinson et al.,
143 2011; Born and Nisancioglu, 2012; Stone et al., 2013). Such scaling is in line with recent
144 studies (e.g. ~~v~~Van de Berg et al., 2013; Merz et al., 2014; Sjolte et al., 2014; Steen-Larsen et
145 al., 2014) that put in question the high temperature of the central estimate reconstructed from
146 the NEEM record. Precipitation rates [for ice sheet forcing](#) vary percentagewise as a function
147 of the $\delta^{18}\text{O}$ record.

148 The AIS forcing is derived directly from the Antarctica Dome C record (EPICA community
149 members, 2004), following again procedures described by Huybrechts (2002). Here,
150 precipitation changes are assumed proportional to the saturated water vapour pressure
151 gradient relative to the temperature above the surface inversion layer. Furthermore, both ice
152 sheet models are forced by changes in global sea-level stand based on the benthic deep-sea
153 record of Lisiecki and Raymo (2005) for the GrIS and on a more recent sea-level

154 reconstruction using Red Sea data (Grant et al., 2012) for the AIS, where the sea-level
155 changes are the dominant forcing. The chronology of the Red Sea record is expected to be
156 more accurate since new dating techniques are applied (Grant et al., 2012). The impact of
157 using another sea-level record for the GrIS simulation over the LIG is small, because of the
158 largely land-based character of the ice sheet during that period. The AIS model is run at a
159 horizontal resolution of 20 x 20 km instead of 10 km x 10 km (as in the standard LOVECLIM
160 configuration and for the GrIS model) due to computational constraints for the relatively long
161 duration of the LIG simulation.

162 To embed the dynamic GrIS simulation in the other NH boundary conditions, the geometric
163 evolution of the GrIS overrides prescribed changes where Greenland ice is present. ~~In that~~
164 ~~ease~~ Therefore, the prescribed ice sheet evolution and associated FWF are not limited by the
165 present-day configuration of the GrIS as in Loutre et al. (2014). The ice sheet evolution is
166 illustrated in Figure 2 for the modelled GrIS embedded in the NH reconstruction (top) and for
167 the modelled AIS (bottom). Ice volume evolution for the NH ice sheets and GrIS and AIS are
168 given in Figure 3a and Figure 3c, respectively. The FWF ~~With from the~~ dynamic GrIS and
169 AIS ~~evolution, their calculated FWF~~ (Figure 3**d**) replace the background freshwater flux
170 from runoff over land calculated by the land model. ~~The ice sheet evolution is illustrated in~~
171 ~~Figure 2 for the modelled GrIS embedded in the NH reconstruction (top) and for the modelled~~
172 ~~AIS (bottom).~~

173 In our setup, the combined sea-level contributions from Antarctica and the NH (including
174 Greenland) fall within the 67% confidence interval of probabilistic sea-level reconstructions
175 (Kopp et al., 2009) for the first peak in sea-level contributions and the following period
176 (~124-120 kyr BP). For both hemispheres, the final 20 m rise in sea-level at the onset of the
177 LIG is however steeper and occurs 1~2 kyr earlier as compared to the reconstructions. When
178 assuming a maximum contribution from glaciers (0.42 ± 0.11) and an additional estimate for
179 thermal expansion of the ocean (0.4 ± 0.3) as given by Masson-Delmotte et al. (2013), the
180 assumed ice sheet evolution in our setup reproduces well the average sea-level contribution
181 between 125 and 120 kyr BP from the best estimate of Kopp et al. (2009), but it does not
182 represent the multi-peak structure of global sea-level contribution during the LIG as suggested
183 by Kopp et al. (2009, 2013). More details about the ice sheet and sea-level evolution can be
184 found in a companion paper (Goelzer et al., 2016) that specifically deals with the sea-level
185 contribution of the ice sheets during the LIG in a fully coupled model set-up.

186 **2.3 Initialisation**

187 The goal of our initialisation technique is to prepare a climate model state for the transient
188 simulations starting at 135 kyr BP that exhibits a minimal coupling drift. Both the GrIS and
189 AIS models are integrated over the preceding glacial cycles and the entire LIG in stand-alone
190 mode. The climate model is then initialized to a steady state with ice sheet boundary
191 conditions, greenhouse gas (GHG) forcing and orbital parameters for the time of coupling
192 (135 kyr BP). In this way, when LOVECLIM is integrated forward in time for transient
193 experiments, the climate component is already relaxed to the ice sheet boundary conditions
194 and exhibits a minimal model drift in unforced control experiments (not shown).

195

196 **3 Experimental setup**

197 All simulations are forced by time-dependent changes in ~~GHG~~greenhouse gas (GHG)
198 concentrations and insolation running from 135 kyr BP until 120 kyr BP (Figure 4). The
199 radiative forcing associated with the reconstructed GHG levels (Petit et al., 1999; Pépin et al.,
200 2001; Raynaud et al., 2005; Loulergue et al., 2008; Spahni et al., 2005) is below preindustrial
201 values for most of this period and barely exceeds it at ~128 kyr BP. The changes in the
202 distribution of insolation received by the Earth are dynamically computed from the changes in
203 the orbital configuration (Berger, 1978) and represent the governing NH forcing during peak
204 LIG conditions aside from evolving ice sheet boundary conditions. In the following, we will
205 compare results of the reference experiment with all ice sheet boundary conditions evolving
206 in time (Reference) to experiments in which the ice sheet boundary conditions are partially
207 fixed to the pre-industrial configuration (Table 1). To disentangle the effects of the individual
208 ice sheets, the experiments noGfwf (suppressed GrIS freshwater fluxes) and noAGfwf
209 (suppressed FWF from both AIS and GrIS) are complemented by two predecessor
210 experiments with fixed AIS and GrIS and evolving NH boundary conditions (noAG), as well
211 as a climate experiment forced by insolation and GHG changes only with all ice sheet
212 boundary conditions fixed (noIS). The latter two experiments correspond to the allLR and
213 IOnly experiments from Loutre et al. (2014).

214

215 **4 Effect of GrIS and AIS on the temperature evolution at the onset of the LIG**

216 ~~As shown by Loutre et al. (2014),~~ including the forcing from the NH ice sheets in terms of
217 configuration and FWF ~~has been shown by Loutre et al. (2014) to be~~ is crucial to simulate the
218 onset of the LIG temperature increase and its amplitude variations ~~with LOVECLIM v.1.3~~
219 more in line with proxy records. This helps to partially overcome problems of EMICs (and
220 general circulation models) to simulate the strong temperature contrasts inferred from proxy
221 reconstructions (Bakker et al., 2013; Lunt et al., 2013). The increased amplitude of
222 temperature changes in our simulations ~~including NH ice sheet boundary conditions~~ is due to
223 albedo and elevation changes in addition to the larger effect of the implied freshwater forcing
224 from the NH ice sheets (Loutre et al., 2014). Here, the Loutre et al. (2014) experiments are
225 complemented with runs that additionally include changes in ice sheet configuration and FWF
226 from the GrIS and AIS. We first discuss the effect of including these additional ice sheet
227 boundary conditions. A specific focus on the FWF follows in section 5.

228 The temperature evolution (Figure 5) before 127 kyr BP is in both hemispheres strongly
229 influenced by the ice sheet boundary conditions and in particular by the freshwater forcing
230 from the ice sheets. The experiments including FWF from the NH ice sheets (Reference and
231 noAG) clearly show temperature variations on the multi-millennial time scale in both
232 hemispheres following variations in ice sheet freshwater input (cf. Figure 3). Differences in
233 the temperature evolution between noAG and the reference experiment are small in the NH,
234 where the additional freshwater flux from Greenland is small compared to the other sources.
235 In the SH, by contrast, a large perturbation arises around 130 kyr BP, when FWF from the
236 AIS peak. Global mean and hemispheric mean temperatures are similar in all runs after ~127
237 kyr BP, when the ice sheets have largely reached their interglacial configuration and ~~their~~
238 FWF are similar between the different experiments. An exception is the GrIS, which is
239 retreating until ~120 kyr BP but accounts for only a small FWF contribution. The similarity of
240 the results in the runs after ~127 kyr BP implies that the temporal memory of the response to
241 ice sheet changes in the system is limited to the multi-centennial time scale, at least for the
242 surface climate. The location of largest freshwater induced temperature variations in the NH
243 is the North Atlantic between 40° N and 80° N. Here changes in the AMOC ~~are the cause for~~
244 a perturbation of the northward oceanic heat transport and temperature changes, which are
245 further amplified by sea ice-albedo and insulation feedbacks. Greenland experiences
246 maximum warming in the reference experiment around 125 kyr BP of up to 2.7°C in the

247 annual mean compared to the pre-industrial over remaining ice covered central Greenland.
248 Here, the temperature evolution is largely similar to the experiment with GrIS changes not
249 accounted for (noAG), which exhibits a maximum warming of 2.4°C (Loutre et al., 2014).
250 However, the summer warming reaches up to 10°C at the northern margin and even up to
251 14°C over southern margins over a then ice-free tundra (not shown). These strong warming
252 trends in the ice sheet periphery is due to a combination of elevation changes and local
253 albedo changes, confined to the immediate region of ice sheet lowering and retreat. In the SH,
254 the largest temperature perturbations linked to both NH and SH freshwater fluxes occur in the
255 SO. The largest warming over the ice sheet itself is simulated over the WAIS (not shown) and
256 is mainly a consequence of the local elevation changes as the ice sheet retreats. However,
257 mainly due to the marine based character of the WAIS, albedo changes are much more limited
258 compared to Greenland as the retreating ice sheet surface is mostly replaced by sea ice.
259 Modelled temperature changes over the East Antarctic ice sheet (EAIS) have been compared
260 to temperature reconstructions for four ice core locations (Figure 6). The reference
261 experiment shows a more pronounced warming between 135 and 129.5 kyr BP compared to
262 the experiments excluding Antarctic ice sheet changes (noAG and noIS). While the modelled
263 warming still appears to be underestimated and delayed compared to the reconstructions, the
264 reference simulation clearly improves the representation of the EAIS temperature evolution
265 compared to experiments with fixed Antarctic boundary conditions.

266

267 **5 Role of ice sheet meltwater fluxes**

268 To study the role of the different freshwater contributions from the ice sheets in more detail
269 and evaluate their importance for the climate evolution, we compare additional simulations
270 where FWF from the GrIS and AIS are partially suppressed relative to the reference
271 experiment (Figure 7). The ice sheet configuration (topography and albedo) remains
272 unchanged in these experiments. The effect of AIS FWF can therefore be evaluated as the
273 difference between noGfwf and noAGfwf, whereas the effect of GrIS FWF becomes apparent
274 from comparing the reference simulation with noGfwf. The AIS FWF (Figure 7f) leads to
275 considerable changes in the Southern HemisphereSH, but has very little impact on the NH
276 temperature evolution (cf. Figure 5b). Conversely, variations in the NH (Figure 7a) and GrIS
277 freshwater forcing on millennial time-scales imply temperature changes in the SH on a
278 background of general LIG warming.

279 Differences between the experiments in the AMOC evolution (Figure 7b) are largely
280 explained by whether FWF from the NH ice sheets and the GrIS are included or not. Here,
281 AMOC strength is calculated as the maximum value of the meridional overturning stream
282 function below the Ekman layer in the Atlantic Ocean between 45° and 65° N. The effect of
283 the FWF from the GrIS (cf. Reference and noGfwf in Figure 7b) is limited compared to the
284 large impact of the general NH ice sheet forcing and consists of an additional weakening of
285 the AMOC. It is most pronounced during periods of AMOC recovery and after 130 kyr BP,
286 when melting of the GrIS beyond its present-day configuration sets in. Note that the
287 simulated evolution of AMOC strength in the reference experiment is in good agreement with
288 paleo evidence based on $\delta^{13}\text{C}$ data (Bauch et al., 2012) and in particular with a recent
289 reconstruction based on chemical water tracers (Böhm et al., 2015). The timing of Heinrich
290 Stadial 11 (~132 kyr BP) and the variations in AMOC strength after that are well captured by
291 our reference simulation, which gives independent credibility to our NH ice sheet
292 reconstructions.

293 The evolution of NH sea ice area (Figure 7c) generally shows maxima at times of AMOC
294 minima and vice versa and is closely linked to NH surface temperature variations (cf. Figure
295 5b) by modifying the heat exchange between ocean and atmosphere. The largest sea ice area
296 between 135 and 130 kyr BP is simulated in the reference experiment, which also exhibits the
297 lowest AMOC strength of all experiments.

298 The situation in the SH is more complex as surface temperature and sea ice evolution are
299 influenced both by freshwater forcing from the AIS as by the FWF in the NH. The AMOC
300 variability gives rise to changes in the SH through the so-called interhemispheric see-saw
301 effect (Stocker 1998). The SH begins to warm as the NH cools due to modified oceanic heat
302 transport across the equator. Minima in SH temperature (cf. Figure 5c) and maxima in SH sea
303 ice area (Figure 7d) are therefore associated with maxima in AMOC strength. The additional
304 effect of including GrIS freshwater forcing is consequently also felt in a warmer SH with less
305 sea ice formation. However, the influence of GrIS freshwater fluxes and consequential
306 AMOC variations on the SH temperature appears to be mostly limited to the beginning of the
307 experiment between ~135 and 131 kyr BP. It could be speculated that this is related to the
308 larger extent of the SH sea ice in a colder climate, making the system more sensitive due to an
309 increased potential for sea ice-albedo and insulation feedbacks. We also note that modelled
310 periods of increased NH freshwater fluxes, reduced AMOC strength and higher SH

311 temperatures are roughly in phase with periods of steeper increase in GHG concentrations (cf.
312 Figure 4b), in line with evidence from marine sediment proxies that indicate that CO₂
313 concentration rose most rapidly when North Atlantic Deep Water shoaled (Ahn and Brook,
314 2008). Since GHGs and NH freshwater fluxes are (independently) prescribed in our
315 experiments, the described in-phase relationship lends further credibility to our NH ice sheet
316 reconstruction.

317 The FWF from AIS melting (Figure 7f) increases the SO sea ice area (Figure 7d) by
318 freshening and stratifying the upper ocean waters, which in turn leads to lower surface
319 temperatures. In our experiments, the increased freshwater flux from the retreating AIS (cf.
320 noGfwf versus noAGfwf) between 131 and 129 kyr BP is in phase with a period of transient
321 AMOC strengthening (Figure 7b), which leads to a combined effect of surface cooling and
322 sea ice expansion in the SO.

323 The formation of AABW is strongly controlled by salinity and sea ice area (and therefore
324 temperature) of the polar surface waters and hence by both Antarctic and indirectly by NH
325 freshwater fluxes. Here, the strength of AABW formation is calculated as the minimum value
326 of the global meridional overturning stream function below the Ekman layer south of 60° S.
327 The AABW formation (Figure 7e) is stronger for saltier and colder surface conditions and
328 therefore strongest in case noAGfwf, where FWF are suppressed from the AIS (saltier) and
329 the GrIS (colder). For a similar Antarctic freshwater forcing, the AABW formation is stronger
330 for a larger SH sea ice area. Including Antarctic FWF leads to a generally weaker AABW
331 formation as surface waters become fresher (cf. noGfwf versus noAGfwf). These
332 relationships imply also that a stronger decrease in AABW formation, associated with
333 decreased CO₂ uptake by the ocean can be found for periods of steeper increase in prescribed
334 radiative forcing. Again, this appears to support consistency in timing between prescribed
335 radiative and NH ice sheet forcing in our modelling.

336

337 **6 Temperature evolution in the Southern Hemisphere**

338 Millennial scale sea-surface temperature variations in the SH induced by NH freshwater
339 fluxes are the strongest in the SO, where anomalies can be amplified by sea ice-albedo and
340 insulation feedbacks. This is also the region that experiences the largest temperature change
341 due to FWF from the AIS itself (not shown).

342 In order to study the effect of Antarctic FWF in more detail, we also analysed the oceanic
343 temperature evolution south of 63°S (Figure 8). The effect of the AIS freshwater flux in the
344 reference experiment (compare noAGfwf with reference) becomes visible in the sea surface
345 temperature after 132 kyr BP (Figure 8a) as a cooling due to stratification and sea ice
346 expansion (Figure 8c). At the same time, the subsurface ocean warms (Figure 8b) as heat is
347 trapped under the stratified surface waters and expanding sea ice area. When the FWF decline
348 towards the end of the AIS retreat around 128 kyr BP, sea ice retreats again and the heat is
349 released to the atmosphere, where it generates an overshoot in SST compared to the
350 experiment with constant Antarctic freshwater fluxes (noAGfwf). The largest effect of this
351 heat buffering is found in winter in regions of strongest warming in the Bellingshausen Sea
352 and off the Gunnerus ridge adjacent to Dronning Maud Land. The maximum sea-ice extent in
353 the SH (Figure 8c) occurs at the time of largest surface cooling at 129.5 kyr BP. This
354 freshwater induced surface cooling at the onset of the LIG appears to be superficial and
355 relatively short lived and of clearly different signature compared to e.g. the Antarctic cold
356 reversal during the last deglaciation. The cooling event is indeed not recorded in our modelled
357 temperature evolution over central East Antarctica, in line with a lack of its signature in
358 Antarctic ice core records for that time period (Petit et al., 1999; EPICA community
359 members, 2004). A sea ice expansion during Termination II together with an *oceanic* cold
360 reversal around 129.5 kyr BP (Figure 8c) is however recorded in some deep-sea sediment
361 cores, where the composition of planktonic diatoms suggests meltwater as the primary cause
362 (Bianchi and Gersonde, 2002; Cortese and Abelmann, 2002).

363 As a further consequence, the timing of maximum annual mean surface air temperature
364 (defined as MWT for Maximum Warmth Timing; Bakker et al., 2013) in the SO differs by
365 several thousand years between experiments (Figure 9). Including Antarctic FWF leads to an
366 earlier MWT (by up to 2 kyr) in large parts of the SO south of 60°S and in the central and
367 eastern parts of the Atlantic sector of the SO up to 40°S (Figure 9d). Conversely, a later MWT
368 (by up to 3 kyr) is found in the Indian and Pacific sectors of the SO north of 60°S when
369 Antarctic FWF is accounted for (Figure 9d). In the reference experiment (Figure 9a) and
370 noGfwf (Figure 9b), the MWT lies relatively homogeneously between -129 kyr and -128 kyr
371 for the entire SO south of 45°S and coincides with the overshoot in SST after the peak input
372 of Antarctic FWF. The observed changes of the MWT in the SO due to the additional
373 Antarctic freshwater input can therefore in either way be understood as a shift towards the
374 time when heat from the mid-depth ocean buffer is released to the surface.

376 **7 Discussion**

377 Despite remaining uncertainties in the timing of ice sheet retreat during Termination II, we
378 find several lines of evidence in support of our ice sheet reconstructions and the associated
379 climatic signatures. The NH ice sheet reconstruction shows some similarity with the IRD
380 signal recorded in North Atlantic sediment cores (Kandiano et al., 2004; Oppo et al., 2006),
381 while the simulated evolution of the AMOC strength (Figure 7a) is in good agreement with a
382 recent reconstruction based on chemical water tracers (Böhm et al., 2015). The combination
383 of NH and SH sourced freshwater forcing variations produces a stronger decrease in AABW
384 formation, associated with decreased CO₂ uptake by the ocean for periods of steeper increase
385 in prescribed radiative forcing, in line with evidence from marine sediment proxies that
386 indicate that CO₂ concentration rose most rapidly when North Atlantic Deep Water shoaled
387 (Ahn and Brook, 2008). Reconstructing the NH ice sheet evolution during Termination II
388 with the same method but using the Grant et al. (2012) sea-level record for comparison with
389 Termination I has been shown to worsen agreement of the modelled climate with proxy
390 reconstructions (Loutre et al., 2014).

391 Our modelling results furthermore suggest that the major AIS retreat from its glacial
392 configuration could be constrained by an oceanic cold event recorded in several SO sediment
393 cores around Antarctica (Bianchi and Gersonde, 2002; Cortese and Abelmann, 2002). As a
394 schematic sensitivity test to uncertainties in the overall glacial AIS volume and retreat rate,
395 we have performed one more experiment identical to the reference experiment except for
396 Antarctic FWF scaled to 50% of their reference value. The resulting magnitude of the SO cold
397 event and overshoot is lower but exhibits the same timing and spatial expression as in the
398 reference case. The described mechanisms and effects can therefore be considered robust to
399 differences in the assumed glacial AIS volumemagnitude of the freshwater flux, resulting
400 from uncertainties in glacial ice volume or AIS retreat rate. Notably, the improved
401 representation of the central East Antarctic temperature evolution in the model when
402 including Antarctic ice sheet changes (Figure 6) is largely independent of the chosen
403 freshwater forcing. This implies that changes in the geometry of the ice sheet and modified
404 atmospheric circulation patterns are the cause for the stronger simulated temperature contrast.

405 The GrIS is generally assumed to have remained largely intact during the LIG (e.g. Robinson
406 et al., 2011; Colville et al., 2011; Stone et al., 2013; NEEM community members, 2013) and

407 indirect evidence of its freshwater contribution may be difficult to find due to the low
408 | amplitude compared to the other ~~NH~~Northern Hemisphere ice sheets. However, recent ice
409 core reconstructions of the temperature evolution at the NEEM ice core site (NEEM
410 community members, 2013) point to a late retreat with a peak sea-level contribution close to
411 | 120 kyr BP. ~~This is the case even if the amplitude of the central estimate of the reconstructed~~
412 ~~temperature anomaly may be debated (e.g. Van de Berg et al., 2013; Merz et al., 2014; Sjolte~~
413 ~~et al., 2014; Steen-Larsen et al., 2014).~~The GrIS can be assumed to lose mass approximately
414 as long as the ~~elimate~~temperature anomaly above the ice sheet remains above zero. Based on
415 the NEEM record, which has been used as forcing time series in our stand-alone GrIS
416 | experiment, FWF from the GrIS peaks at ~125 kyr BP, but remains elevated until around 120
417 kyr BP above the steady state background flux of an ice sheet in equilibrium with the climate.
418 The additional FWF from melting of the GrIS results in relatively low temperatures over
419 Southeast Greenland in response to a weakening of the AMOC (not shown). The interaction
420 between GrIS meltwater fluxes and oceanic circulation hence give rise to a negative feedback
421 on ice sheet retreat. This aspect could play an important role for the stability of the southern
422 dome of the ice sheet and should be examined further with fully coupled climate-ice sheet
423 simulations.

424 In general, the NH freshwater forcing leads to variations in the strength of the AMOC and
425 North Atlantic cooling and additionally through the bipolar see-saw effect, to temperature
426 changes in the SH. The only moment mid-depth ocean temperatures close to AIS grounding
427 lines are above pre-industrial values in our experiments is during the oceanic cold reversal
428 around 129.5 kyr BP, induced by anomalous FWF from the retreating AIS. During this
429 period, SO mid-depth temperature anomalies relative to the pre-industrial reach up to 0.3 K,
430 which could provide a positive but rather limited feedback on ice sheet retreat, similar to what
431 has been suggested by Golledge et al. (2014) for meltwater pulse 1A during Termination I.
432 However, the oceanic warming recorded in our model is not strong and the duration of the
433 perturbation does not appear to be long enough for a sustained impact on the retreat of the ice
434 sheet. Furthermore, the peak in freshwater flux appears when the ice sheet has already
435 retreated considerably and WAIS grounding lines are located mostly on the continental
436 shelves, more protected from the warm water build-up in the mid-depth ocean. A large-scale
437 marine ice sheet retreat of the likely less vulnerable EAIS sectors (Mengel and Levermann,
438 2014) appears particularly unlikely, given the atmospheric and oceanic forcing at the time

439 apparent in our modelling results. However, in-depth studies of these interactions require
440 detailed coupled simulations of the entire ocean-ice sheet system.

441 Despite aforementioned lines of evidence in support of the reconstructed NH ice sheet
442 evolution, a limitation to our modelling approach is the rescaling of ~~post-LGM-NH~~ ice sheet
443 retreat during Termination I, an attempt to address the sparseness of geomorphological field
444 evidence for Termination II. An alternative approach would be to physically model all ice
445 sheets together in one framework (e.g. de Boer et al. 2013), although spatial and temporal
446 resolution of the models is a limiting factor in that specific case. A rigorous modelling
447 approach like the latter could also help to prevent possible inconsistencies when combining
448 ice sheet reconstructions from different approaches. Nevertheless, any modelling approach
449 will ultimately be confronted with the same problem of scarce data for model validation
450 during that period. The exclusion of climate feedbacks on ice sheet evolution of our present
451 one-way coupled modelling approach is a general limitation, which we have addressed in a
452 separate study with a fully coupled model set-up (Goelzer et al., 2016).

453

454 **8 Conclusion**

455 We have presented a transient simulation of Termination II and the Last Interglacial period
456 with realistic ice sheet boundary conditions from reconstructed ~~NH~~Northern Hemisphere ice
457 sheets and detailed stand-alone simulations of the Greenland and Antarctic ice sheets. Our
458 results show that the temperature evolution at the onset of the Last Interglacial was in both
459 hemispheres considerably influenced by meltwater fluxes from the retreating ice sheets.
460 While Antarctic freshwater fluxes lead to strong perturbations of the Southern Ocean,
461 ~~Northern Hemisphere~~NH freshwater fluxes have an influence both on the Northern and
462 ~~Southern Hemisphere~~SH temperature evolution through the oceanic see-saw effect. The
463 importance of additional freshwater input from the GrIS during Termination II is small
464 compared to the much larger fluxes from the other NH ice sheets and becomes more
465 important only later during the Interglacial when it is the only remaining ice sheet
466 contributing freshwater fluxes to the North Atlantic. In the ~~Southern Hemisphere~~SH,
467 anomalous freshwater input from the AIS leads to an episode of surface freshening, increased
468 stratification and sea ice cover and consequently reduced ocean heat loss to the atmosphere,
469 with temporary heat build-up in the mid-depth ocean. We argue that the surface ocean cooling

470 associated with this event may be used to constrain an early Antarctic retreat when matched
471 with similar signatures evident in some deep-sea sediment cores from the Southern Ocean.

472 Our transient simulations confirm results from earlier studies that stress the importance of ice
473 sheet boundary conditions for the climate evolution at the onset of the LIG. However, most of
474 the freshwater induced changes remain visible for at most 1-2 kyr after cessation of the
475 perturbations, indicative of a relative short memory of the (surface) climate system.
476 Additional effects may arise from climate-ice sheet feedbacks not considered in the present
477 model configuration, which should be investigated in fully-coupled experiments.

478

479 **Appendix A: Reconstruction of NH ice sheet forcing**

480 A direct reconstruction of NH ice sheet evolution during Termination II based on
481 geomorphological data is not possible, due to the scarcity of field evidence that was mostly
482 destroyed by the re-advancing ice sheets during the last glacial period. Therefore, a
483 reconstruction of Termination II is made by remapping the much better constrained ice sheet
484 post-LGM retreat of Termination I.

485 **Post-LGM ice extent during Termination I**

486 The evolution of the northern-hemisphere NH ice extent since the LGM was estimated based
487 on published sources (Table A1) dating back to the time of the NH ice sheet studies of Zweck
488 and Huybrechts (2003, 2005). For the large Laurentide and Eurasian ice sheets inferred ice
489 extents are relatively well determined from geomorphological data and the reconstruction
490 remains in good agreement with most recent sources (e.g. Hughes et al. 2016). For smaller ice
491 sheets such as the European Alps previous modelled ice extent was used (Zweck and
492 Huybrechts, 2005).

493 For ice sheets with multiple sources of data the isochrones were merged using the more-most
494 recent source when conflicts occurred (e.g. Dyke et al. (2002) instead of Dyke and Prest
495 (1987) for the Innuitian ice sheet, Svendsen et al. (1999) instead of Andersen (1981) for the
496 LGM maximum of the Eurasian ice sheet). The more-most recent source was then used as a
497 mask of maximum ice extent for more-most recent isochrones of all sources. The only region,
498 which experienced an advance in post-LGM ice extent using this technique was the southern
499 Cordilleran ice sheet according to the reconstruction of Clague and James (2002+).

500 The INTCAL98 timescale of Stuiver et al. (1998) was used to convert radiocarbon dates to
501 calendar years for the sources in Table A1. The retreat of the ice sheets between the LGM and
502 PD was prescribed at 200 year resolution. Even for well-determined geomorphological
503 observations, uncertainties in dating and from the conversion ~~from-of~~ radiocarbon to calendar
504 years well exceed the 200 year temporal resolution used here. Figure A1 shows the
505 deglaciation chronology reconstructed in this manner.

506 IPost-LGM ice sheet elevations during Termination I

507 The ~~northern hemisphere~~NH ice sheets introduced significant changes to the surface
508 topography of the region. As LOVECLIM1.3 has only 3 atmospheric height levels, details
509 regarding topography are not strongly sensed. To include changes in surface topography in
510 the model, parabolic profile ice sheets are constructed using the extents shown in Figure A1,
511 ~~assuming conditions of no isostatic adjustment~~neglecting isostatic adjustment (i.e. present-
512 day surface elevation of the Earth's surface). ~~The basal shear stress for the parabolic profile~~
513 ~~reconstruction is chosen so that the difference in ice volume between LGM and PD~~
514 ~~corresponds to 86 m of eustatic sea level change.~~ ~~This value is chosen so that were isostasy~~
515 ~~accounted for an additional 24 m of ice would produce a similar elevation and contribute a~~
516 ~~total equivalent eustatic sea level change of 110 m, in keeping with the results for the~~
517 ~~Northern Hemisphere ice sheets since the LGM of Zweck and Huybrechts (2005)~~With
518 isostasy accounted for, a similar elevation would result in an additional contribution of 24 m
519 to a total equivalent eustatic sea level change of 110 m (cf. Zweck and Huybrechts, 2005). ~~τ~~
520 Using this procedure the maximum elevation of the Laurentide ice sheet is 3000 m near
521 present-day Churchill in Hudson Bay, and the maximum elevation of the Eurasian ice sheet
522 is 2600 m 100 km west of present-day Helsinki.

523 Remapping Termination I post-LGM retreat to Termination II

524 Remapping of the ~~post-LGM~~retreat during Termination I to Termination II is done using a
525 benthic $\delta^{18}\text{O}$ record (Lisiecki and Raymo, 2005), assumed as an indicator of the global ice
526 volume. In practice, the NH ice sheet configuration for a given time (and $\delta^{18}\text{O}$ value) during
527 Termination II is taken from a time during Termination I ~~the post-LGM retreat~~ when the $\delta^{18}\text{O}$
528 value had the same value. The LGM sea-level contribution of the NH ice sheets relative to the
529 present day of -110 m translates into a similar magnitude for the penultimate glacial
530 maximum (Lisiecki and Raymo, 2005). The resulting NH ice volume evolution for
531 Termination II is shown in Figure 3a. However, the method does not guarantee that the sea-

532 level contribution of the reconstructed NH ice sheets closely follows the global ice volume
533 curve. This is generally due to the mismatch between global ice volume and NH ice sheet
534 reconstruction during ~~the post-LGM period~~Termination I, and in part related to the
535 unconstrained contribution of other components (AIS, thermal expansion). Due to the
536 assumed analogy, different configurations of the N~~orthern Hemisphere~~ ice sheets (e.g.
537 Obrochta et al., 2014) and different relative timing of NH and SH deglaciation between last
538 and penultimate glaciation are not represented in these reconstructions. NH freshwater fluxes
539 were estimated from the same method by using derived volume changes as input to a
540 continental runoff routing model (Goelzer et al., 2012b) to identify the magnitude and
541 location of meltwater fluxes to the ocean.

542
543

544 **9 Acknowledgements**

545 We acknowledge support through the Belgian Federal Science Policy Office within its
546 Research Programme on Science for a Sustainable Development under contract SD/CS/06A
547 (iCLIPS). Computational resources have been provided by the supercomputing facilities of
548 the Université catholique de Louvain (CISM/UCL) and the Consortium des Equipements de
549 Calcul Intensif en Fédération Wallonie Bruxelles (CECI) funded by the Fond de la Recherche
550 Scientifique de Belgique (FRS-FNRS). We thank two anonymous reviewers and the editor for
551 constructive comments and their follow-up of the manuscript.

552

553 **10 References**

- 554 Ahn, J., and Brook, E.: Atmospheric CO₂ and climate on millennial time scales during the last
555 glacial period, *Science*, 322, 83-85, doi: 10.1126/science.1160832 2008.
- 556 Andersen, B. G.: Late Weichselian ice sheets in Eurasia and Greenland, in: *The Last Great Ice*
557 *Sheets*, edited by: Denton, G. H., and Hughes, T. J., Wiley Interscience, New York, 1 - 65,
558 1981.
- 559 Bakker, P., Stone, E. J., Charbit, S., Gröger, M., Krebs-Kanzow, U., Ritz, S. P., Varma, V.,
560 Khon, V., Lunt, D. J., Mikolajewicz, U., Prange, M., Renssen, H., Schneider, B., and Schulz,
561 M.: Last interglacial temperature evolution – a model inter-comparison, *Clim.*
562 *Past.*, 9, 605-619, doi:10.5194/cp-9-605-2013, 2013.
- 563 Barker, S., Knorr, G., Edwards, R. L., Parrenin, F., Putnam, A. E., Skinner, L. C., Wolff, E.,
564 and Ziegler, M.: 800,000 Years of Abrupt Climate Variability, *Science*, 334, 347-351,
565 doi:10.1126/science.1203580 2011.
- 566 Bauch, H. A., Kandiano, E. S., and Helmke, J. P.: Contrasting ocean changes between the
567 subpolar and polar North Atlantic during the past 135 ka, *Geophys. Res. Lett.*, 39, L11604,
568 doi:10.1029/2012GL051800, 2012.
- 569 Berger, A.: Long-term variations of daily insolation and Quaternary climatic changes, *Journal*
570 *of Atmospheric Sciences*, 35, 2362-2367, doi:10.1175/1520-
571 0469(1978)035<2362:LTVODI>2.0.CO;2, 1978.
- 572 Bianchi, C., and Gersonde, R.: The Southern Ocean surface between Marine Isotope Stages 6
573 and 5d: Shape and timing of climate changes, *Palaeogeography, Palaeoclimatology,*
574 *Palaeoecology*, 187, 151-177, doi:10.1016/S0031-0182(02)00516-3, 2002.
- 575 Bintanja, R., Van Oldenborgh, G. J., Drijfhout, S. S., Wouters, B., and Katsman, C. A.:
576 Important role for ocean warming and increased ice-shelf melt in Antarctic sea-ice expansion,
577 *Nat. Geosci.*, 6, 376-379, doi:10.1038/ngeo1767, 2013.
- 578 Böhm, E., Lippold, J., Gutjahr, M., Frank, M., Blaser, P., Antz, B., Fohlmeister, J., Frank, N.,
579 Andersen, M. B., and Deininger, M.: Strong and deep Atlantic meridional overturning
580 circulation during the last glacial cycle, *Nature*, 517, 73–76 doi:10.1038/nature14059, 2015.
- 581 Born, A., and Nisancioglu, K. H.: Melting of Northern Greenland during the last
582 interglaciation, *Cryosphere*, 6, 1239-1250, doi:10.5194/tc-6-1239-2012, 2012.

583 Brovkin, V., Ganopolski, A., and Svirezhev, Y.: A continuous climate-vegetation
584 classification for use in climate-biosphere studies, *Ecol. Model.*, 101, 251-261,
585 doi:10.1016/S0304-3800(97)00049-5, 1997.

586 Capron, E., Govin, A., Stone, E. J., Masson-Delmotte, V., Mulitza, S., Otto-Bliesner, B.,
587 Rasmussen, T. L., Sime, L. C., Waelbroeck, C., and Wolff, E. W.: Temporal and spatial
588 structure of multi-millennial temperature changes at high latitudes during the Last
589 Interglacial, *Quat. Sci. Rev.*, 103, 116-133, doi:10.1016/j.quascirev.2014.08.018, 2014.

590 Clague, J. J., and James, T. S.: History and isostatic effects of the last ice sheet in southern
591 British Columbia, *Quat. Sci. Rev.*, 21, 71-87, doi:10.1016/s0277-3791(01)00070-1, 2002.

592 Colville, E. J., Carlson, A. E., Beard, B. L., Hatfield, R. G., Stoner, J. S., Reyes, A. V., and
593 Ullman, D. J.: Sr-Nd-Pb Isotope Evidence for Ice-Sheet Presence on Southern Greenland
594 During the Last Interglacial, *Science*, 333, 620-623, doi:10.1126/science.1204673, 2011.

595 Cortese, G., and Abelmann, A.: Radiolarian-based paleotemperatures during the last 160 kyr
596 at ODP Site 1089 (Southern Ocean, Atlantic Sector), *Palaeogeography, Palaeoclimatology,*
597 *Palaeoecology*, 182, 259-286, doi:10.1016/S0031-0182(01)00499-0, 2002.

598 de Boer, B., van de Wal, R. S. W., Lourens, L. J., Bintanja, R., and Reerink, T. J.: A
599 continuous simulation of global ice volume over the past 1 million years with 3-D ice-sheet
600 models, *Clim. Dyn.*, 41, 1365-1384, doi:10.1007/s00382-012-1562-2, 2013.

601 Driesschaert, E., Fichet, T., Goosse, H., Huybrechts, P., Janssens, I., Mouchet, A.,
602 Munhoven, G., Brovkin, V., and Weber, S.: Modeling the influence of Greenland ice sheet
603 melting on the Atlantic meridional overturning circulation during the next millennia,
604 *Geophys. Res. Lett.*, 34, 10707, doi:10.1029/2007GL029516, 2007.

605 Duplessy, J. C., Roche, D. M., and Kageyama, M.: The deep ocean during the last interglacial
606 period, *Science*, 316, 89-91, doi:10.1126/science.1138582, 2007.

607 Dutton, A., and Lambeck, K.: Ice Volume and Sea Level During the Last Interglacial,
608 *Science*, 337, 216-219, doi:10.1126/science.1205749, 2012.

609 Dyke, A. S., Andrews, J. T., Clark, P. U., England, J., Miller, G. H., Shaw, J., and Veillette, J.
610 J.: The Laurentide and Innuitian ice sheets during the Last Glacial Maximum, *Quat. Sci. Rev.*,
611 21, 9-31, doi:10.1016/S0277-3791(01)00095-6, 2002.

612 Dyke, A. S., and Prest, V. K.: Late Wisconsinan and Holocene history of the Laurentide Ice
613 Sheet, *Géog. Phys. Quat.*, 41, 237 - 263, doi:10.7202/032681ar, 1987.

614 EPICA community members: Eight glacial cycles from an Antarctic ice core, *Nature*, 429,
615 623-628, doi:10.1038/Nature02599, 2004.

616 Fürst, J. J., Goelzer, H., and Huybrechts, P.: Ice-dynamic projections of the Greenland ice
617 sheet in response to atmospheric and oceanic warming, *The Cryosphere*, 9, 1039-1062,
618 doi:10.5194/tc-9-1039-2015, 2015.

619 Goelzer, H., Huybrechts, P., Loutre, M. F., Goosse, H., Fichefet, T., and Mouchet, A.: Impact
620 of Greenland and Antarctic ice sheet interactions on climate sensitivity, *Clim. Dyn.*, 37, 1005-
621 1018, doi:10.1007/s00382-010-0885-0, 2011.

622 Goelzer, H., Huybrechts, P., Raper, S. C. B., Loutre, M. F., Goosse, H., and Fichefet, T.:
623 Millennial total sea level commitments projected with the Earth system model of intermediate
624 complexity LOVECLIM, *Environ. Res. Lett.*, 7, doi:10.1088/1748-9326/7/4/045401, 2012a.

625 Goelzer, H., Janssens, I., Nemeč, J., and Huybrechts, P.: A dynamic continental runoff
626 routing model applied to the last Northern Hemisphere deglaciation, *Geosci. Model Dev.*, 5,
627 599-609, doi:10.5194/gmd-5-599-2012, 2012b.

628 Goelzer, H., Huybrechts, P., Loutre, M.-F., and Fichefet, T.: Last Interglacial climate and sea-
629 level evolution from a coupled ice sheet-climate model, *Clim. Past. Discuss.*, in review,
630 doi:10.5194/cp-2015-175, 2016.

631 Golledge, N. R., Menviel, L., Carter, L., Fogwill, C. J., England, M. H., Cortese, G., and
632 Levy, R. H.: Antarctic contribution to meltwater pulse 1A from reduced Southern Ocean
633 overturning, *Nature Communications*, 5, doi:10.1038/ncomms6107, 2014.

634 Goosse, H., and Fichefet, T.: Importance of ice-ocean interactions for the global ocean
635 circulation: A model study, *J. Geophys. Res.*, 104, 23337-23355, doi:10.1029/1999JC900215,
636 1999.

637 Goosse, H., Brovkin, V., Fichefet, T., Haarsma, R., Huybrechts, P., Jongma, J., Mouchet, A.,
638 Selten, F., Barriat, P.-Y., Campin, J.-M., Deleersnijder, E., Driesschaert, E., Goelzer, H.,
639 Janssens, I., Loutre, M. F., Morales Maqueda, M. A., Opsteegh, T., Mathieu, P.-P.,
640 Munhoven, G., Pettersson, E. J., Renssen, H., Roche, D. M., Schaeffer, M., Tartinville, B.,
641 Timmermann, A., and Weber, S. L.: Description of the Earth system model of intermediate

642 complexity LOVECLIM version 1.2, *Geosci. Model Dev.*, 3, 603-633, doi:10.5194/gmd-3-
643 603-2010, 2010.

644 Govin, A., Braconnot, P., Capron, E., Cortijo, E., Duplessy, J. C., Jansen, E., Labeyrie, L.,
645 Landais, A., Marti, O., Michel, E., Mosquet, E., Risebrobakken, B., Swingedouw, D., and
646 Waelbroeck, C.: Persistent influence of ice sheet melting on high northern latitude climate
647 during the early Last Interglacial, *Clim. Past.*, 8, 483-507, doi:10.5194/cp-8-483-2012, 2012.

648 Grant, K. M., Rohling, E. J., Bar-Matthews, M., Ayalon, A., Medina-Elizalde, M., Ramsey,
649 C. B., Satow, C., and Roberts, A. P.: Rapid coupling between ice volume and polar
650 temperature over the past 150,000 years, *Nature*, 1-4, doi:10.1038/nature11593, 2012.

651 Greve, R., Saito, F., and Abe-Ouchi, A.: Initial results of the SeaRISE numerical experiments
652 with the models SICOPOLIS and IcIES for the Greenland ice sheet, *Ann. Glaciol.*, 52, 23-30,
653 doi:10.3189/172756411797252068, 2011.

654 Holden, P., Edwards, N. R., Wolff, E., Lang, N., Singarayer, J., Valdes, P., and Stocker, T.:
655 Interhemispheric coupling, the West Antarctic Ice Sheet and warm Antarctic interglacials,
656 *Clim. Past.*, 6, 431-443, doi:10.5194/cp-6-431-2010, 2010.

657 Hughes, A. L. C., Gyllencreutz, R., Lohne, Ø. S., Mangerud, J., and Svendsen, J. I.: The last
658 Eurasian ice sheets – a chronological database and time-slice reconstruction, *DATED-1*,
659 *Boreas*, 45, 1-45, doi:10.1111/bor.12142, 2016.

660 Huybrechts, P.: A 3-D model for the Antarctic Ice Sheet: a sensitivity study on the glacial-
661 interglacial contrast, *Clim. Dyn.*, 5, 79-92, doi:10.1007/BF00207423, 1990.

662 Huybrechts, P.: Sea-level changes at the LGM from ice-dynamic reconstructions of the
663 Greenland and Antarctic ice sheets during the glacial cycles, *Quat. Sci. Rev.*, 21, 203-231,
664 doi:10.1016/S0277-3791(01)00082-8, 2002.

665 Kandiano, E. S., Bauch, H. A., and Müller, A.: Sea surface temperature variability in the
666 North Atlantic during the last two glacial–interglacial cycles: comparison of faunal, oxygen
667 isotopic, and Mg/Ca-derived records, *Palaeogeography, Palaeoclimatology, Palaeoecology*,
668 204, 145-164, doi:10.1016/S0031-0182(03)00728-4, 2004.

669 Kopp, R. E., Simons, F. J., Mitrovica, J. X., Maloof, A. C., and Oppenheimer, M.:
670 Probabilistic assessment of sea level during the last interglacial stage, *Nature*, 462, 863-867,
671 doi:10.1038/nature08686, 2009.

672 Kopp, R. E., Simons, F. J., Mitrovica, J. X., Maloof, A. C., and Oppenheimer, M.: A
673 probabilistic assessment of sea level variations within the last interglacial stage, *Geophys. J.*
674 *Int.*, 193, 711-716, doi:10.1093/gji/ggt029, 2013.

675 Landvik, J. Y., Bondevik, S., Elverhøi, A., Fjeldskaar, W., Mangerud, J., Salvigsen, O.,
676 Siegert, M. J., Svendsen, J. I., and Vorren, T. O.: The Last Glacial Maximum of Svalbard and
677 the Barents Sea area: ice sheet extent and configuration, *Quat. Sci. Rev.*, 17, 43-75,
678 doi:10.1016/S0277-3791(97)00066-8, 1998.

679 Langebroek, P. M., and Nisancioglu, K. H.: Simulating last interglacial climate with
680 NorESM: role of insolation and greenhouse gases in the timing of peak warmth, *Clim. Past.*,
681 10, 1305-1318, doi:10.5194/cp-10-1305-2014, 2014.

682 | Letréguilly, A., Huybrechts, P., and Reeh, N.: Steady-state characteristics of the Greenland
683 ice sheet under different climates, *J. Glaciol.*, 37, 149-157, 1991.

684 Lisiecki, L. E., and Raymo, M. E.: A Pliocene-Pleistocene stack of 57 globally distributed
685 benthic delta O-18 records, *Paleoceanography*, 20, 17, doi:10.1029/2004pa001071, 2005.

686 Loulergue, L., Schilt, A., Spahni, R., Masson-Delmotte, V., Blunier, T., Lemieux, B.,
687 Barnola, J.-M., D. Raynaud, Stocker, T. F., and Chappellaz, J.: Orbital and millennial-scale
688 features of atmospheric CH₄ over the past 800,000 years, *Nature*, 453, 383-386,
689 doi:10.1038/nature06950, 2008.

690 Loutre, M. F., Fichet, T., Goosse, H., Huybrechts, P., Goelzer, H., and Capron, E.: Factors
691 controlling the last interglacial climate as simulated by LOVECLIM1.3, *Clim. Past.*, 10,
692 1541-1565, doi:10.5194/cp-10-1541-2014, 2014.

693 Lunt, D. J., Abe-Ouchi, A., Bakker, P., Berger, A., Braconnot, P., Charbit, S., Fischer, N.,
694 Herold, N., Jungclauss, J. H., Khon, V. C., Krebs-Kanzow, U., Langebroek, P. M., Lohmann,
695 G., Nisancioglu, K., Otto-Bliesner, B., Park, W., Pfeiffer, M., Phipps, S. J., Prange, M.,
696 Rachmayani, R., Renssen, H., Rosenbloom, N., Schneider, B., Stone, E. J., Takahashi, K.,
697 Wei, W., Yin, Q., and Zhang, Z. S.: A multi-model assessment of last interglacial
698 temperatures, *Clim. Past.*, 9, 699-717, doi:10.5194/cp-9-699-2013, 2013.

699 Mangerud, J., Astakhov, V., and Svendsen, J. I.: The extent of the Barents-Kara Ice Sheet
700 during the Last Glacial Maximum, *Quat. Sci. Rev.*, 21, 111-119, doi:10.1016/s0277-
701 3791(01)00088-9, 2002.

702 Marino, G., Rohling, E. J., Rodriguez-Sanz, L., Grant, K. M., Heslop, D., Roberts, A. P.,
703 Stanford, J. D., and Yu, J.: Bipolar seesaw control on last interglacial sea level, *Nature*, 522,
704 197-201, doi:10.1038/nature14499, 2015.

705 Masson-Delmotte, V., Buiron, D., Ekaykin, A., Frezzotti, M., Gallée, H., Jouzel, J., Krinner,
706 G., Landais, A., Motoyama, H., Oerter, H., Pol, K., Pollard, D., Ritz, C., Schlosser, E., Sime,
707 L. C., Sodemann, H., Stenni, B., Uemura, R., and Vimeux, F.: A comparison of the present
708 and last interglacial periods in six Antarctic ice cores, *Clim. Past.*, 7, 397-423,
709 doi:10.5194/cp-7-397-2011, 2011.

710 Masson-Delmotte, V., Schulz, M., Abe-Ouchi, A., Beer, J., Ganopolski, A., González Rouco,
711 J., Jansen, E., Lambeck, K., Luterbacher, J., Naish, T., Osborn, T., Otto-Bliesner, B., T.
712 Quinn, R. R., M. Rojas, X. S., and Timmermann, A.: Information from paleoclimate archives,
713 in: *Climate Change 2013: The Physical Science Basis. Contribution of Working Group I to*
714 *the Fifth Assessment Report of the Intergovernmental Panel on Climate Change*, edited by:
715 Stocker, T. F., Qin, D., Plattner, G.-K., Tignor, M., Allen, S. K., Boschung, J., Nauels, A.,
716 Xia, Y., Bex, V., and Midgley, P. M., Cambridge University Press, , Cambridge, United
717 Kingdom and New York, NY, USA, 383-464, 2013.

718 Mayewski, P., Denton, G., and Hughes, T.: Late Wisconsin Ice Sheets in North America, in:
719 *The Last Great Ice Sheets*, edited by: Denton, G., and Hughes, T., Wiley Interscience, New
720 York, 67-178, 1981.

721 Mengel, M., and Levermann, A.: Ice plug prevents irreversible discharge from East
722 Antarctica, *Nature Climate Change*, 4, 451-455, doi:10.1038/nclimate2226, 2014.

723 Menviel, L., Timmermann, A., Timm, O. E., and Mouchet, A.: Deconstructing the Last
724 Glacial termination: the role of millennial and orbital-scale forcings, *Quat. Sci. Rev.*, 30,
725 1155-1172, doi:10.1016/j.quascirev.2011.02.005, 2011.

726 Merz, N., Born, A., Raible, C. C., Fischer, H., and Stocker, T. F.: Dependence of Eemian
727 Greenland temperature reconstructions on the ice sheet topography, *Clim. Past*, 10, 1221-
728 1238, doi:10.5194/cp-10-1221-2014, 2014.

729 NEEM community members: Eemian interglacial reconstructed from a Greenland folded ice
730 core, *Nature*, 493, 489-494, doi:10.1038/nature11789, 2013.

731 Obrochta, S. P., Crowley, T. J., Channell, J. E. T., Hodell, D. A., Baker, P. A., Seki, A., and
732 Yokoyama, Y.: Climate variability and ice-sheet dynamics during the last three glaciations,
733 *Earth Planet. Sci. Lett.*, 406, 198-212, doi:10.1016/j.epsl.2014.09.004, 2014.

734 Oppo, D. W., McManus, J. F., and Cullen, J. L.: Evolution and demise of the Last Interglacial
735 warmth in the subpolar North Atlantic, *Quat. Sci. Rev.*, 25, 3268-3277,
736 doi:10.1016/j.quascirev.2006.07.006, 2006.

737 Opsteegh, J. D., Haarsma, R. J., Selten, F. M., and Kattenberg, A.: ECBILT: a dynamic
738 alternative to mixed boundary conditions in ocean models, *Tellus*, 50, 348-367,
739 doi:10.1034/j.1600-0870.1998.t01-1-00007.x, 1998.

740 | Péepin, L., Raynaud, D., Barnola, J. M., and Loutre, M. F.: Hemispheric roles of climate
741 forcings during glacial-interglacial transitions as deduced from the Vostok record and LLN-
742 2D model experiments, *J. Geophys. Res. [Atmos.]*, 106, 31885-31892,
743 doi:10.1029/2001jd900117, 2001.

744 Petit, J.-R., Jouzel, J., Raynaud, D., Barkov, N. I., Barnola, J.-M., Basile, I., Bender, M.,
745 Chappellaz, J., Davis, M. E., Delaygue, G., Delmotte, M., Kotlyakov, V. M., Legrand, M.,
746 Lipenkov, V. Y., Lorius, C., Pepin, L., Ritz, C., Saltzman, E., and Stievenard, M.: Climate
747 and atmospheric history of the past 420,000 years from the Vostok ice core, *Antarctica*,
748 *Nature*, 399, 429-436, doi:10.1038/20859, 1999.

749 Raynaud, D., Barnola, J. M., Souchez, R., Lorrain, R., Petit, J. R., Duval, P., and Lipenkov,
750 V. Y.: Palaeoclimatology - The record for marine isotopic stage 11, *Nature*, 436, 39-40,
751 doi:10.1038/43639b, 2005.

752 Robinson, A., Calov, R., and Ganopolski, A.: Greenland ice sheet model parameters
753 constrained using simulations of the Eemian Interglacial, *Clim. Past.*, 7, 381-396,
754 doi:10.5194/cp-7-381-2011, 2011.

755 | ~~Sanchez-Goni~~ **Sánchez Goñi**, M. F., Bakker, P., Desprat, S., Carlson, A. E., Van Meerbeeck,
756 C. J., Peyron, O., Naughton, F., Fletcher, W. J., Eynaud, F., Rossignol, L., and Renssen, H.:
757 European climate optimum and enhanced Greenland melt during the Last Interglacial,
758 *Geology*, 40, 627-630, doi:10.1130/G32908.1 2012.

759 Sjolte, J., and Hoffmann, G.: Modelling stable water isotopes in monsoon precipitation during
760 the previous interglacial, *Quat. Sci. Rev.*, 85, 119-135, doi:10.1016/j.quascirev.2013.12.006,
761 2014.

762 Spahni, R., Chappellaz, J., Stocker, T. F., Loulerge, L., Hausammann, G., Kawamura, K.,
763 Flückiger, J., Schwander, J., Raynaud, D., Masson-Delmotte, V., and Jouzel, J.: Atmospheric
764 methane and nitrous oxide of the late Pleistocene from Antarctic ice cores, *Science*, 310,
765 1317-1321, doi:10.1126/science.1120132 2005.

766 Steen-Larsen, H. C., Masson-Delmotte, V., Hirabayashi, M., Winkler, R., Satow, K., Prié, F.,
767 Bayou, N., Brun, E., Cuffey, K. M., Dahl-Jensen, D., Dumont, M., Guillevic, M., Kipfstuhl,
768 S., Landais, A., Popp, T., Risi, C., Steffen, K., Stenni, B., and Sveinbjörnsdóttir, A. E.: What
769 controls the isotopic composition of Greenland surface snow?, *Clim. Past.*, 10, 377-392,
770 doi:10.5194/cp-10-377-2014, 2014.

771 Stocker, T. F.: The Seesaw Effect, *Science*, 282, 61-62, doi:10.1126/science.282.5386.61,
772 1998.

773 Stocker, T. F., and Johnsen, S. J.: A minimum thermodynamic model for the bipolar seesaw,
774 *Paleoceanography*, 18, 1087, doi:10.1029/2003PA000920, 2003.

775 Stone, E. J., Lunt, D. J., Annan, J. D., and Hargreaves, J. C.: Quantification of the Greenland
776 ice sheet contribution to Last Interglacial sea level rise, *Clim. Past.*, 9, 621-639,
777 doi:10.5194/cp-9-621-2013, 2013.

778 [Stuiver, M., Reimer, P. J., Bard, E., Beck, J. W., Burr, G. S., Hughen, K. A., Kromer, B.,](#)
779 [McCormac, G., van der Plicht, J., and Spurk, M.: INTCAL98 radiocarbon age calibration,](#)
780 [24,000-0 cal BP, *Radiocarbon*, 40, 1041-1083, 1998.](#)

781 Svendsen, J. I., Alexanderson, H., Astakhov, V. I., Demidov, I., Dowdeswell, J. A., Funder,
782 S., Gataullin, V., Henriksen, M., Hjort, C., Houmark-Nielsen, M., Hubberten, H. W.,
783 Ingolfsson, O., Jakobsson, M., Kjær, K. H., Larsen, E., Lokrantz, H., Lunkka, J. P., Lyså, A.,
784 Mangerud, J., Matiouchkov, A., Murray, A., Möller, P., Niessen, F., Nikolskaya, O., Polyak,
785 L., Saarnisto, M., Siegert, C., Siegert, M. J., Spielhagen, R., and Stein, R.: Late Quaternary
786 ice sheet history of northern Eurasia, *Quat. Sci. Rev.*, 23, 1229-1271,
787 doi:10.1016/j.quascirev.2003.12.008, 2004.

788 Svendsen, J. I., Astakhov, V. I., Bolshiyakov, D. Y., Demidov, I., Dowdeswell, J. A.,
789 Gataullin, V., Hjort, C., Hubberten, H. W., Larsen, E., Mangerud, J., Melles, M., Möller, P.,
790 Saarnisto, M., and Siegert, M. J.: Maximum extent of the Eurasian ice sheets in the Barents
791 and Kara Sea region during the Weichselian, *Boreas*, 28, 234-242, doi:10.1111/j.1502-
792 3885.1999.tb00217.x, 1999.

793 Swingedouw, D., Fichefet, T., Huybrechts, P., Goosse, H., Driesschaert, E., and Loutre, M.
794 F.: Antarctic ice-sheet melting provides negative feedbacks on future climate warming,
795 *Geophys. Res. Lett.*, 35, L17705, doi:10.1029/2008GL034410, 2008.

796 Turney, C. S. M., and Jones, R. T.: Does the Agulhas Current amplify global temperatures
797 during super-interglacials?, *J. Quat. Sci.*, 25, 839-843, doi:10.1002/jqs.1423, 2010.

798 van de Berg, W. J., van den Broeke, M. R., van Meijgaard, E., and Kaspar, F.: Importance of
799 precipitation seasonality for the interpretation of Eemian ice core isotope records from
800 Greenland, *Clim. Past.*, 9, 1589-1600, doi:10.5194/cp-9-1589-2013, 2013.

801 Zweck, C., and Huybrechts, P.: Modeling the marine extent of northern hemisphere ice sheets
802 | during the last glacial cycle, *Ann. Glaciol.*, 37, 173-180, [doi:10.3189/172756403781815870](https://doi.org/10.3189/172756403781815870),
803 2003.

804 Zweck, C., and Huybrechts, P.: Modeling of the northern hemisphere ice sheets during the
805 last glacial cycle and glaciological sensitivity, *J. Geophys. Res.*, 110, D07103,
806 doi:10.1029/2004JD005489, 2005.

807

808

809

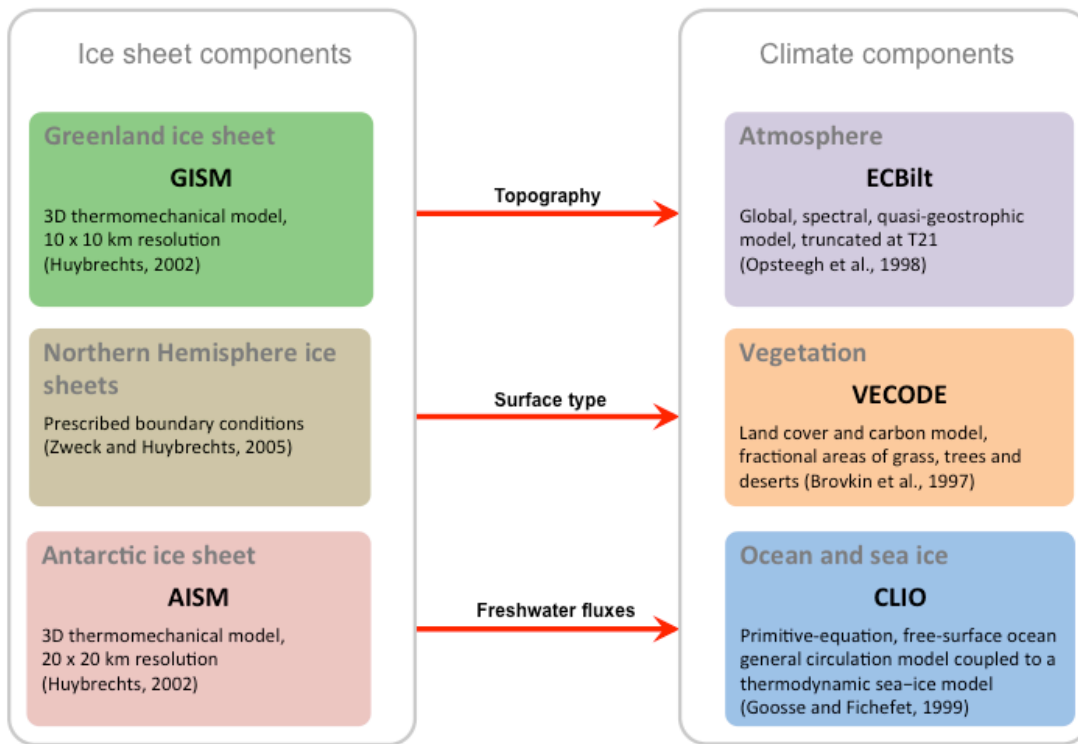
810 **11 Tables**

811

812 **Table 1: Matrix of all experiments and the respective ice sheet components that evolve in time (yes) or are**
 813 **fixed (no). In the latter case, freshwater fluxes (FWF, grey) are kept constant and topography and surface**
 814 **albedo are fixed to the preindustrial configuration.**

EXP	topo NH	FWF NH	topo GrIS	FWF GrIS	topo AIS	FWF AIS
Reference	yes	yes	yes	yes	yes	yes
noGfwf	yes	yes	yes	no	yes	yes
noAGfwf	yes	yes	yes	no	yes	no
noAG	yes	yes	no	no	no	no
noIS	no	no	no	no	no	no

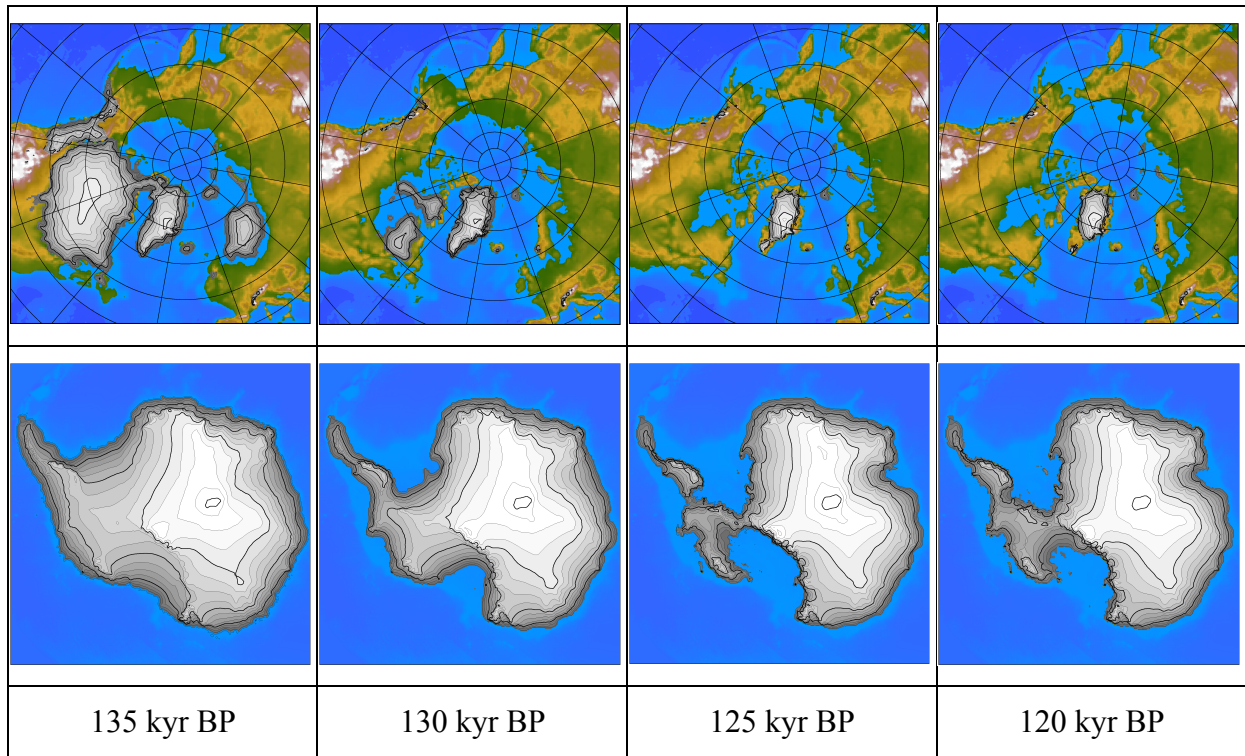
815



817

818 **Figure 1: LOVECLIM model setup for the present study including prescribed ice sheet boundary**
 819 **conditions from the Northern Hemisphere, Greenland and Antarctic ice sheets.**

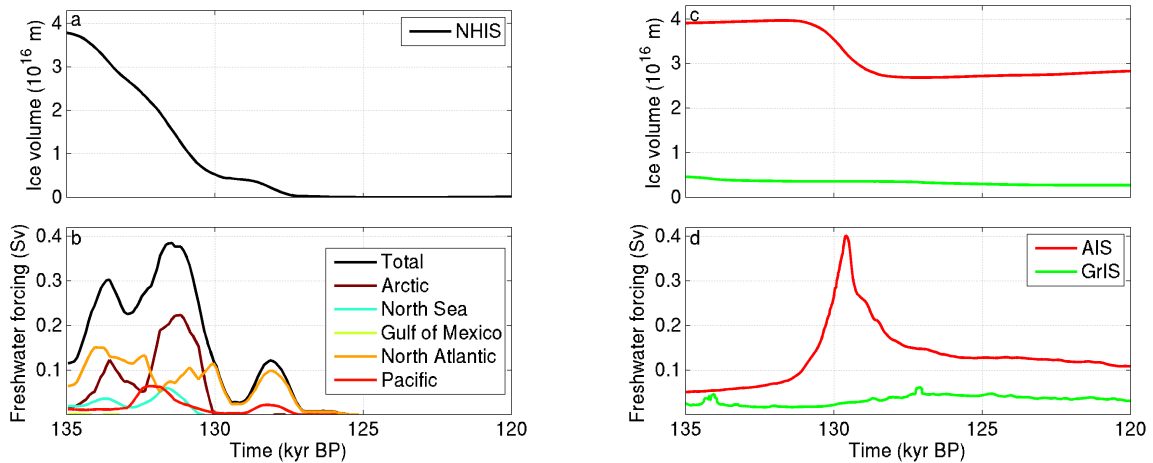
820



822 **Figure 2: Evolution of reconstructed Northern Hemisphere ice sheets and embedded modelled GrIS (top)**
 823 **and modelled AIS (bottom) used as boundary conditions for the climate model.**

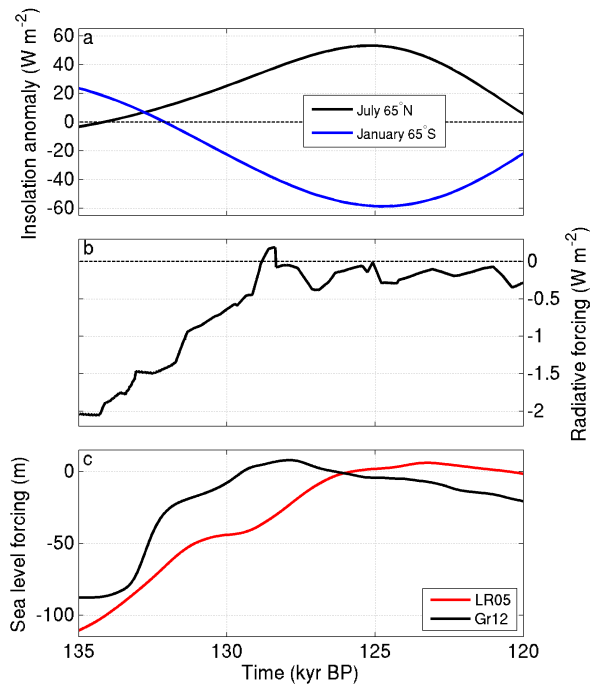
824

825

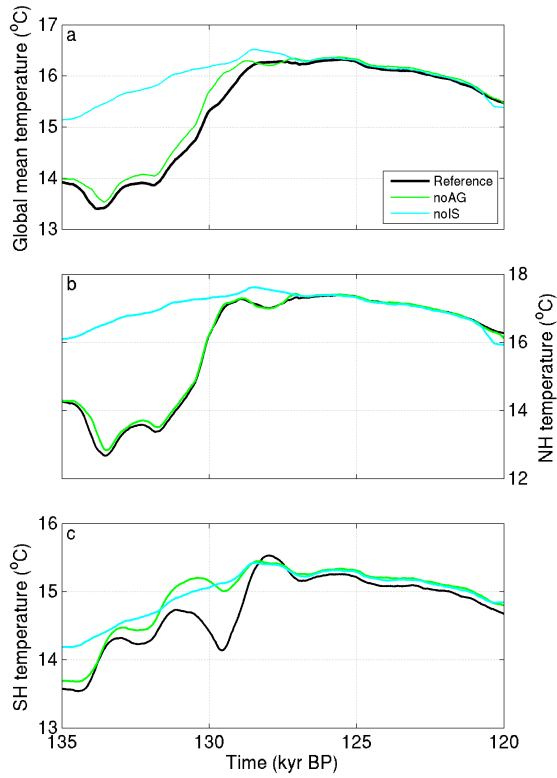


826 **Figure 3: Reconstructed ice volume (a, c) and freshwater forcing (b, d) from the NH ice sheets (left) and**
 827 **from the GrIS and AIS (right). See Goelzer et al. (2012b) for definition of oceanic basins in panel b.**

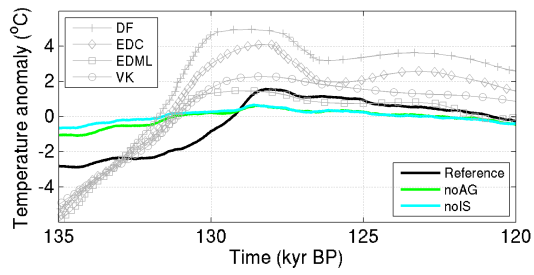
828



829 **Figure 4: Prescribed model forcings. (a) Average monthly insolation anomaly relative to the pre-industrial**
 830 **at 65° North in July (black) and 65° South in January (blue). (b) combined radiative forcing anomaly of**
 831 **prescribed greenhouse gas concentrations (CO₂, CH₄, N₂O) relative to the pre-industrial. (c) sea-level**
 832 **forcing for the ice sheet components derived from either oceanic δ¹⁸O data (Lisiecki and Raymo, 2005,**
 833 **red) scaled to a global sea-level contrast between LGM and present day of 130 m or derived from a Red**
 834 **Sea relative sea-level record (Grant et al. 2012, black).**
 835



837 **Figure 5: Evolution of global mean (a), northern (b) and southern (c) hemispheric mean surface**
 838 **temperature for experiments with different ice sheet forcing included. Curves are smoothed with a**
 839 **running mean of 200 years for better comparison.**
 840



841

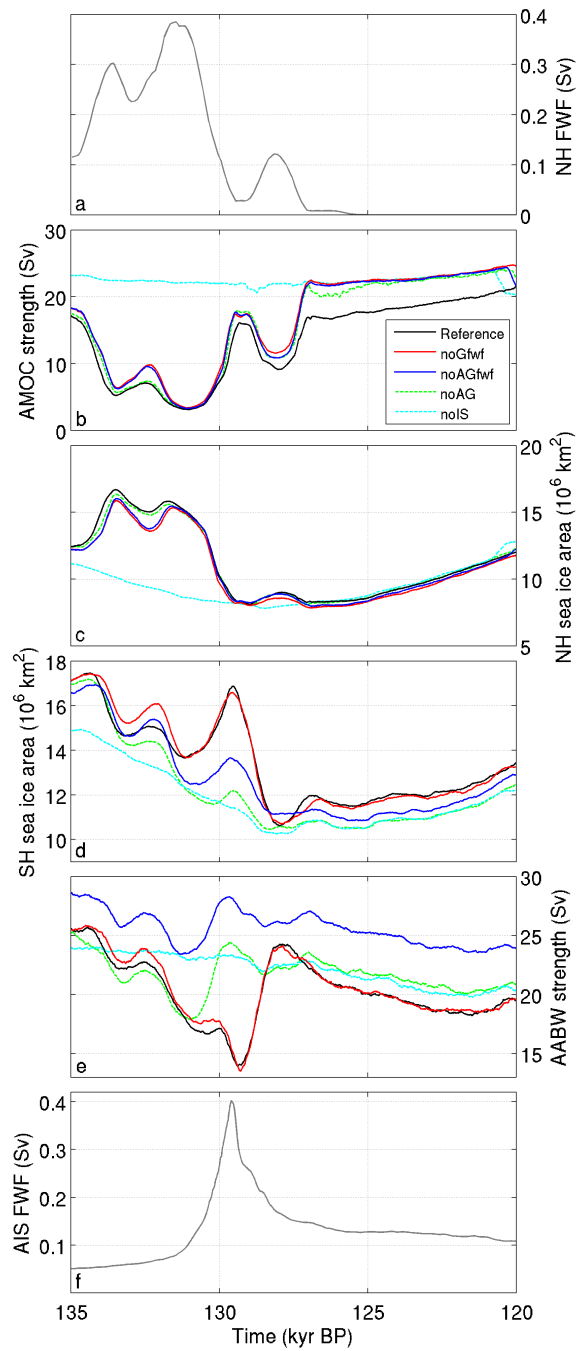
842 **Figure 6: Comparison of modelled East Antarctic temperature evolution with reconstructed temperature**

843 **changes at deep ice core sites. Modelled temperature anomalies are averaged over a region 72° - 90° S and**

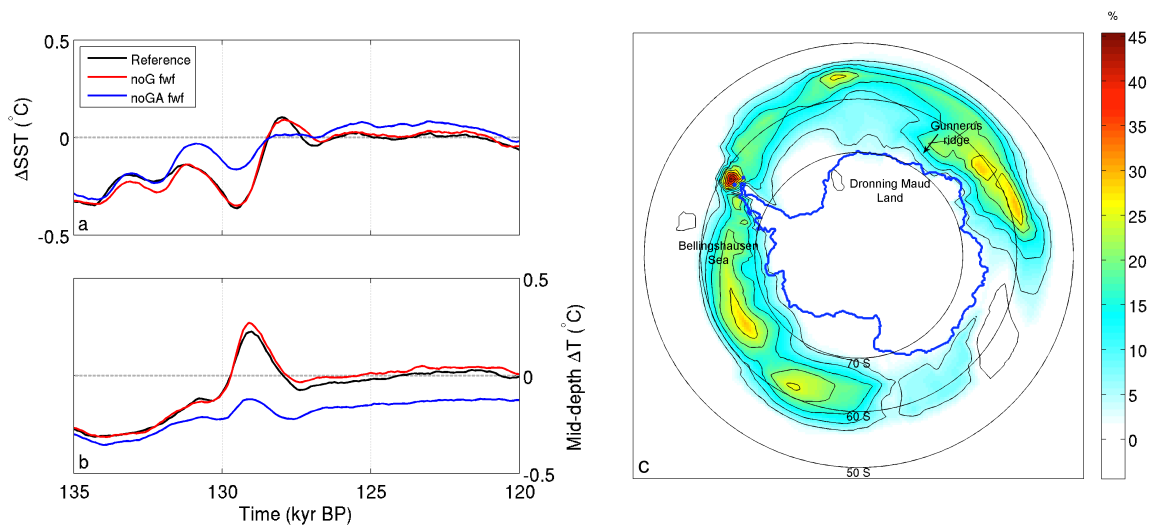
844 **0° - 150° E. Ice core temperature reconstructions for the sites EPICA Dronning Maud Land (EDML,**

845 **75°00' S, 00°04' E), Dome Fuji (DF, 77°19' S, 39°40' E), Vostok (VK, 78°28' S, 106°48' E) and EPICA**

846 **Dome C (EDC, 75°06' S, 123°21' E) are from Masson-Delmotte et al. (2011).**



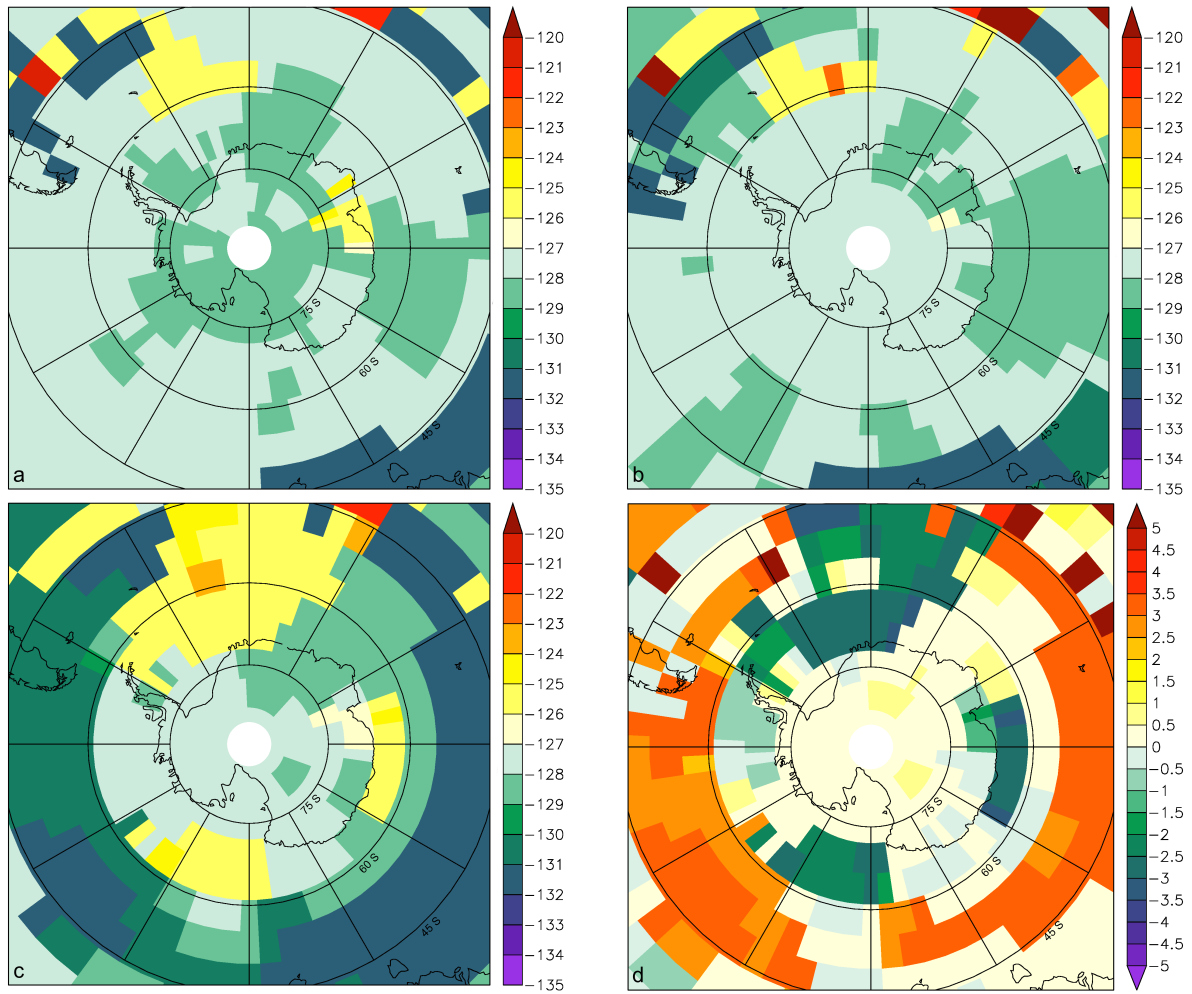
847 **Figure 7: Freshwater forcing and oceanic response characteristics. NH (a) and Antarctic ice sheet**
 848 **freshwater fluxes (f), strength of the AMOC (b), NH sea ice area (c), SH sea ice area (d) and strength of**
 849 **AABW formation (e) for the different experiments with and without freshwater forcing from Greenland,**
 850 **Antarctic and NH ice sheet melting. Curves are smoothed with a running mean of 200 years for better**
 851 **comparison.**
 852



853 **Figure 8: Evolution of annual mean sea surface temperature (a) and mid-depth (485-700 m) ocean**
 854 **temperature (b) anomalies relative to the pre-industrial in close proximity to the AIS (south of 63°S). (c)**
 855 **Meltwater related changes in annual mean sea ice area at 129.5 kyr BP from differences between**
 856 **experiments Reference and noAGfwf in per cent. The blue contour outlines the observed ice-shelf edge**
 857 **and grounded ice margin of the present-day AIS for illustration. All curves (a, b) are smoothed with a**
 858 **running mean of 200 years for better comparison.**

859

860



861

862 **Figure 9: Time of maximum surface air temperature (MWT) in kyr BP for experiments Reference (a),**

863 **noGfwf (b) and noAGfwf (c) and difference in MWT between experiments noGfwf and noAGfwf (d) in**

864 **kyr, showing the shift of the MWT when Antarctic freshwater fluxes are included.**

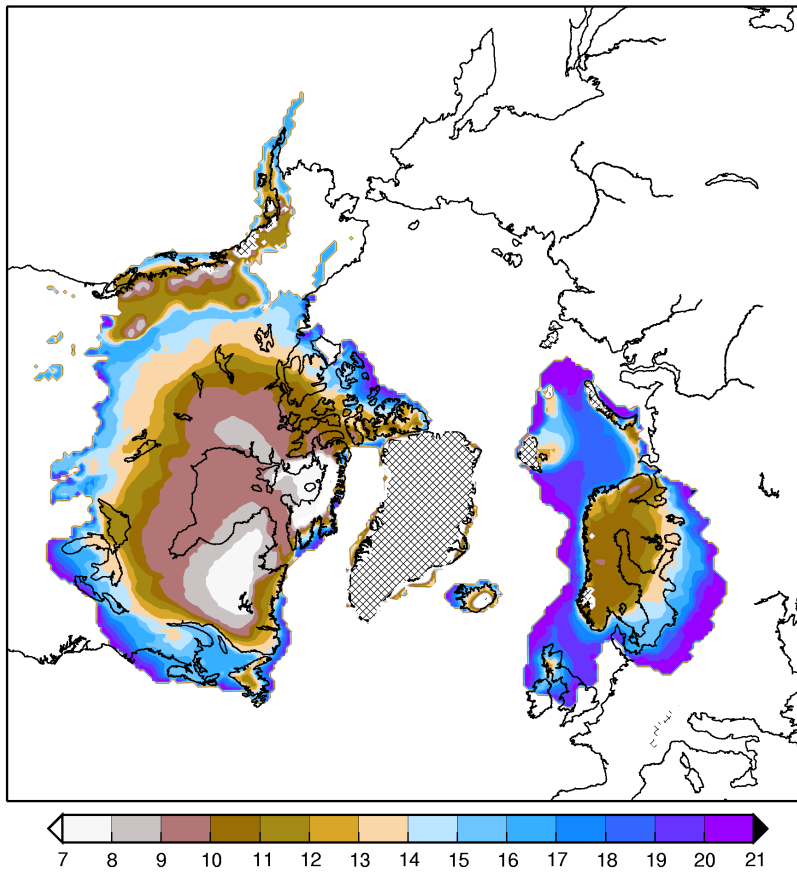
865

866

867 **Table A1: Sources of geomorphological data or modelling results used to prescribe changes in Northern**
 868 **Hemisphere ice sheet extent for the post-LGM retreat during Termination I.**

Ice Sheet	Source	Isochrone Time Period (kyr BP)
Laurentide	Dyke and Prest (1987)	18 – Present Day
Innuitian	Dyke et al. (2002)	18
Cordilleran	Clague and James (2002 ⁴) Dyke et al. (2002) Mayewski et al. (1981)	20 – Present Day (south) 18 (north) 21 – 7 (interior)
Iceland	Andersen (1981)	20 – Present Day
Eurasian	Andersen (1981) Landvik et al. (1998) Mangerud et al. (2002) Svendsen et al. (1999)	20 – Present Day 15 – 12 (Barents Sea) 18 (Southern Barents and Kara Seas) 18
European Alps	Zweck and Huybrechts (2003 ²)	21 – Present Day (modelled ice extent)

869



870

871

872

Figure A1: Interpolated ice sheet extent during the last deglaciation for the Northern Hemisphere ice sheets as a function of time (kyr BP). Hatched regions indicate present-day ice.